CrystEngComm

Accepted Manuscript

ROYAL SOCIETY OF CHEMISTRY

www.rsc.org/crystengcomm

Table of contents

Hydrogen-Bonding Patterns in a Series of Multi-component Molecular Solids Formed by 2,3,5,6-Tetramethylpyrazine with Selected Carboxylic Acids

Lei Wang[a*], Ruiyu Xue[a], Yuanxin Li[a], Yiran Zhao[a], Faqian Liu[a], and Keke Huang[b*]

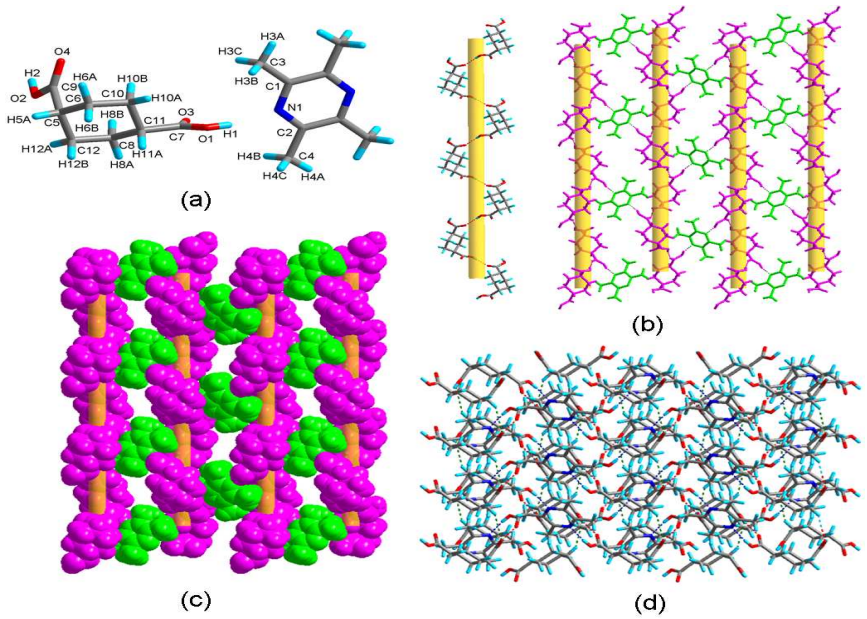

Hydrogen-Bonding Patterns in a Series of Cocrystals of 2,3,5,6-Tetramethylpyrazine with Selected Carboxylic Acids were discussed in the context.

CrystEngComm RSCPublishing

ARTICLE

Hydrogen-Bonding Patterns in a Series of Multi-component Molecular Solids Formed by 2,3,5,6-Tetramethylpyrazine with Selected Carboxylic Acids

Cite this: DOI: 10.1039/x0xx00000x

Received 00th January 201x,
Accepted 00th January 201x

DOI: 10.1039/x0xx00000x

www.rsc.org/

Lei Wang[a*], Ruiyu Xue[a], Yuanxin Li[a], Yiran Zhao[a], Faqian Liu[a], and Keke Huang[b*]

The analysis of noncovalent interactions in several complexes constructed by 2,3,5,6-tetramethylpyrazine with different acid ligands, 1,4-cyclohexanedicarboxylic acid, 2,6-dihydroxybenzoic acid, 2,6-pyridinedicarboxylic acid, 6-hydroxy-2-naphthoic acid, 3-nitrophthalic acid, o-phthalic acid and 3-hydroxybenzoic acid, supported by single crystal X-ray diffraction analysis is presented. It reveals that all of these forms except **2** are organic supramolecular cocrystals without charge-transfer between multicomponent acids and the base. Noncovalent interactions directed assemblies of the eight structures are managed by classical O-H···O, O-H···N, weak C-H···O and π-π stacking interactions to generate 2D or 3D supermolecular architectures. For **5**, **6**, **7** and **8**, carboxyl/pyrazine supramolecular heterosynthons $R^2_2(6)$ and $R^2_2(8)$ containing classical O-H···N and weak C-H···O interactions, usually observed in organic cocrystals of carboxylic acid and heterocyclic base, is again confirmed to participate in constructing these hydrogen-bonding supermolecular networks. In addition, weak C-H···O interactions were involved in building and consolidating their structures in all organic complexes. The thermal stability of crystals 1-8 has been investigated by thermogravimetric analysis (TGA) of mass loss.

Introduction

Noncovalent intermolecular forces have received considerable attention in the design and synthesis of various types of organic solid materials[1], including hydrates[2], solvate[3], cocrystals[4,5] and salts[5]. Among these supramolecular interactions, charge-assisted[6] or neutral hydrogen bonds, π-π stacking, van der Waals interactions, electrostatic interactions, etc, which are widely known to form a series of supramolecular synthons[7], the hydrogen bonds are the most unquestionably efficient tool in view of their selectivity and directionality[8] in the field of organic crystal designing. Not only stronger classical hydrogen bonds (O-H···O, O-H···N, etc.)[9], but also weaker interactions such as C-H···X (X=π, O, N, F, etc.)[10] play significant roles in designing of well-defined supramolecular assemblies. However, it remains a central challenge in successfully controlling the assembly of these noncovalent interactions to obtain the desired supramolecular entities because of the relatively weak hydrogen-bonding accepting ability and reversible nature[11].

As far as we know, numerous carboxylic acids have been generally utilized in the synthesizing organic cocrystals/salts or coordination polymers[12], for their carboxyl functional group can be used to form abundant supramolecular synthons though strong and directional hydrogen bonds. Meantime, a variety of basic building blocks such as pyrazines, pyridines, amines and their analogues were documented in the past few years[13]. As a excellent ligand, pyrazine ring is a planar structure, and the carbons are sp^2 hybridization. Therefore, pyrazine is more likely to form 2D hydrogen-bonded networks[8a,14]. However, compared with pyrazine, 2,3,5,6-tetramethylpyrazine molecule is larger because of its four methyl-arms, and the carbons of methyl are sp^3 hybridization which can provide more potential C-H···X hydrogen-bonds to form 3D supramolecular framework with diverse structures and properties. In our previous study[15], N,N'-dimethylpiperazine has been applied as molecular building block to construct a series of organic salt with

[a] *College of Chemistry and Molecular Engineering, Qingdao University of Science and Technology, Qingdao 266042, P. R. China. E-mail: inorchemwl@126.com; Fax: (+86) 532-840-22681*
[b] *State Key Laboratory of Inorganic Synthesis and Preparative Chemistry, Jilin University, Changchun, 130012, PR China. E-mail: kkhuang@jlu.edu.cn;*

† Electronic Supplementary Information (ESI) available: IR. CCDC reference numbers 987037-987044. For ESI and crystallographic data in CIF or other electronic format see DOI:XXXXXXXXX

aromatic multicomponent acids[15g]. The piperazine ring of *N,N'*-dimethylpiperazine is saturated, having no aromaticity. Besides, the aqueous solution of *N,N'*-dimethylpiperazine is alkaline. Thence, the N atom of piperazine ring has a tendency to be protonated and *N,N'*-dimethylpiperazine is more likely to form organic salts with acidic molecules[16]. While aromatic 2,3,5,6-tetramethylpyrazine is a weaker base than *N,N'*-dimethylpiperazine. By comparison with pyrazine and *N,N'*-dimethylpiperazine, 2,3,5,6-tetramethylpyrazine could be more likely to build 3D supramolecular cocrystals theoretically which can be predictted[17]. In previous work, several examples had been reported, illustrating the importance and influence of such supramolecular building blocks to establish intriguing supramolecular assemblies[18]. However, much systematic work in this area still needs to be done.

With this background, in this paper, we focus on the ability of 2,3,5,6-tetramethylpyrazine and carboxylic acids to form supramolecular homo- or heterosynthons for the sake of exploring the hydrogen bonding formation and molecular recognition in supramolecular synthesis and continuing of our work. Consequently we chose 2,3,5,6-tetramethylpyrazine and the following coformers that contain multifunctional groups (therefore forming multiple supramolecular synthons): 1,4-cyclohexanedicarboxylic acid, 2,6-dihydroxybenzoic acid, 2,6-pyridinedicarboxylic acid, 6-hydroxy-2-naphthoic acid, 3-nitrophthalic acid, o-phthalic acid and 3-hydroxybenzoic acid, (Scheme 1**)** as building blocks. A series of multi-component molecular solids including seven cocrystals and one salt of 2,3,5,6-tetramethylpyrazine with carboxylic acids were prepared: $[(C_8H_{12}O_4)\cdot(C_8H_{12}N_2)_{0.5}]$**(1)**, **[**$(C_7H_6O_4)_2\cdot(C_7H_5O_4)^-\cdot(C_8H_{13}N_2)^+\cdot(C_8H_{12}N_2)_{0.5}$**](2)**, $[(C_7H_5NO_5)\cdot(C_8H_{12}N_2)_{0.5}\cdot H_2O]$**(3)**, $[(C_{11}H_8O_3)_2\cdot(C_8H_{12}N_2)]$**(4)**, $[(C_8H_5NO_6)\cdot(C_8H_{12}N_2)_{0.5}\cdot H_2O]$**(5)**, $[(C_8H_6O_4)\cdot(C_8H_{12}N_2)]$**(6)**, $[(C_8H_6O_4)\cdot(C_8H_{12}N_2)_{0.5}]$**(7)**, $[(C_7H_6O_3)\cdot(C_8H_{12}N_2)_{1.5}]$**(8)**.

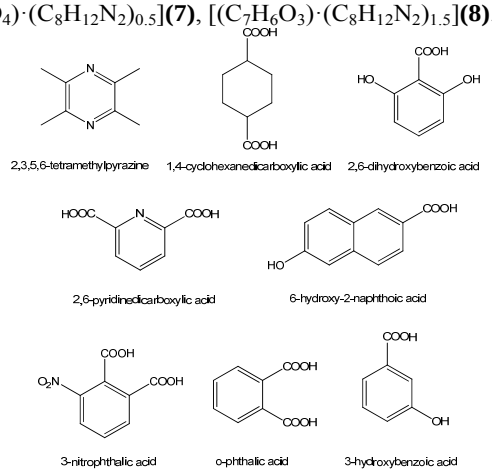

Scheme 1 Molecular Components Used in Crystallization**.**

Experimental section

General materials and methods

All reagents were analytical grade and received from commercial sources without further purification. Melting points of the new compounds were determined on a WRS-1B digital thermal apparatus without correction, and elemental (C, H, and N) analyses were performed on a Perkin-Elmer 2400 elemental analyzer. Fourier transform infrared (FT-IR) spectra (KBr pellets) were measured on a Nicolet Impact 410 FTIR spectrometer in the range 4000-400cm^{-1}. Thermogravimetric analysis (TGA) experiments were taken on a Perkin-Elmer 7 thermogravimetric analyzer from 25 to 900 °C under nitrogen atmosphere at a heating rate of 10 °C /min.

Syntheses of the Cocrystal 1-8

Synthesis of $[(C_8H_{12}O_4)\cdot(C_8H_{12}N_2)_{0.5}]$ (1) A mixture of 1,4-cyclohexanedicarboxylic acid (0.0344 g, 0.2 mmol) and 2,3,5,6-tetramethylpyrazine (0.0136 g, 0.1 mmol) were dissolved in an ethanol-water solution (1 : 1 v/v, 10 mL) with constant stirring until a clear, homogeneous solution was obtained. Colorless lamellar crystals were harvested after 3 weeks with slow evaporation of the solvents in air. Yield: 79%. Anal. Calcd for $C_{12}H_{18}NO_4$ (%): C, 60.00; H, 7.50; N, 5.83. Found (%): C, 59.35; H, 7.93; N, 5.39. IR(cm^{-1}): 2959s, 2861s, 2736m, 2681m, 2613m, 1698s, 1454m, 1421m, 1319s, 1266s, 1202s, 1041w, 950s, 915m, 898m, 754m, 683w, 644w, 523m, 449w.

Synthesis of $[(C_7H_6O_4)_2\cdot(C_7H_5O_4)^-\cdot(C_8H_{13}N_2)^+\cdot(C_8H_{12}N_2)_{0.5}]$ (2) The same procedure as that for **1** was used except for the introduction of 2,6-dihydroxybenzoic acid (0.0376 g, 0.2 mmol) instead of 1,4-cyclohexanedicarboxylic acid. Colorless block crystals were collected in yield 81% after 2 weeks at room temperature. Anal. Calcd for $C_{22}H_{24}N_2O_8$ (%): C, 59.46; H, 5.40; N, 6.31. Found (%): C, 58.92; H, 5.81; N, 6.03. IR(cm^{-1}): 3056w, 2997w, 2788w, 2732w, 2162w, 2060w, 1979w, 1641s, 1583s, 1526m, 1447s, 1393s, 1343m, 1295m, 1200s, 1157m, 1137m, 1119w, 1064w, 1031s, 997w, 827s, 768m, 745m, 707m, 673w, 611w, 575w, 530w, 486w.

Synthesis of $[(C_7H_5NO_5)\cdot(C_8H_{12}N_2)_{0.5}\cdot H_2O]$ (3) 2,6-Pyridinedicarboxylic acid (0.0334 g, 0.2 mmol) was dissolved in hot water (5 mL), to which an ethanol solution (5 mL) of 2,3,5,6-tetramethylpyrazine (0.0272 g, 0.2 mmol) was added. The reaction mixture was filtered after constant stirring for 20 min and allowed to evaporate in air for 2 weeks. Colorless block crystals suitable for X-ray analysis were obtained in 75% yield. Anal. Calcd for $C_{11}H_{13}N_2O_5$ (%): C, 52.17; H, 5.14; N, 11.07. Found (%): C, 51.92; H, 5.61; N, 10.82. IR(cm^{-1}): 3412s, 3093w, 2920w, 2792w, 2627w, 1954w, 1732s, 1651w, 1579w, 1450w, 1387m, 1308s, 1267s, 1175m, 1080m, 996m, 885w, 848w, 769w, 751s, 721w, 693m, 647w, 562w, 528w, 493w, 437w.

Synthesis of $[(C_{11}H8_5O_3)\cdot(C_8H_{12}N_2)]$ (4) 6-Hydroxy-2-naphthoic acid (0.0376 g, 0.2 mmol) and 2,3,5,6-tetramethylpyrazine (0.0545 g, 0.4 mmol) were mixed and dissolved in an ethanol-water solution (1 : 1 v/v, 10 mL) with constant stirring. Colorless block single crystals suitable for X-ray analysis appeared after 4 weeks at room temperature. Yield: 80%. Anal. Calcd for $C_{30}H_{28}N_2O_6$ (%): C, 70.31; H, 5.47; N, 5.47. Found (%): C, 69.91; H, 5.73; N, 5.63. IR(cm^{-1}): 3440s, 2923w, 2861w, 1629m, 1448w, 1413w, 1202w, 1181w, 990w, 436w, 417w.

Synthesis of $[(C_8H_5NO_6)\cdot(C_8H_{12}N_2)_{0.5}\cdot H_2O]$ (5) 3-Nitrophthalic acid (0.0422 g, 0.2 mmol) and 2,3,5,6-tetramethylpyrazine (0.0272 g, 0.2 mmol) were mixed and dissolved in an acetone-water solution (1 : 1 v/v, 10 mL) with constant stirring. The resultant clear solution was

left standing under ambient conditions .With slow evaporation of the solvents, colorless lamellar crystals were produced after 3 weeks. Yield: 76%. Anal. Calcd for $C_{12}H_{13}N_2O_7$ (%): C, 48.48; H, 4.38; N, 9.43. Found (%): C, 48.06; H, 4.82; N, 9.27. IR(cm^{-1}): 3440m, 2872m, 2787m, 2598m, 2509m, 2176w, 2079w, 1720s, 1569m, 1534s, 1466m, 1396m, 1351s, 1272s, 1200m, 1122m, 1072m, 997m, 910m, 853w, 780m, 748m, 695m, 667m, 620w, 576w, 534w .

Synthesis of $[(C_8H_6O_4)\cdot(C_8H_{12}N_2)]$ (6) An ethanol solution (5 mL) of o-phthalic acid (0.0332 g, 0.2 mmol) was added to a tetrahydrofuran solution (5 mL) of 2,3,5,6-tetramethylpyrazine (0.0545 g, 0.4 mmol) with constant stirring for 15 min. The resultant colorless solution was left to stand at room temperature, affording colorless block crystals after 21 days in 83% yield. Anal. Calcd for $C_{12}H_{13}N_2O_7$ (%): C, 63.58; H, 5.96; N, 9.27. Found (%): C, 62.97; H, 6.27; N, 8.95. IR(cm^{-1}): 3435m, 2922m, 2591m, 1903w, 1694s, 1599w, 1489w, 1381w, 1364w, 1311m, 1073w, 991w, 944w, 829w, 800w, 747m, 688w, 673w, 643w, 587w, 553w, 475w.

Synthesis of $[(C_8H_6O_4)\cdot(C_8H_{12}N_2)_{0.5}]$ (7) O-phthalic acid (0.0332 g, 0.2 mmol) and 2,3,5,6-tetramethylpyrazine (0.0272 g, 0.2 mmol) were mixed and dissolved in an ethanol-water solution (1 : 1 v/v, 10 mL) with constant stirring. The resultant colorless solution was allowed to stand at room temperature, and block single crystals suitable for X-ray diffraction were obtained by evaporation of the solvents within 3 week in 81% yield. Anal. Calcd for $C_{12}H_{12}NO_4$ (%): C, 61.54; H, 5.13; N, 5.98. Found (%): C, 61.21; H, 5.48; N, 5.67. IR(cm^{-1}): 3435m, 3065m, 3006m, 2880m, 2651m, 2525w, 1691s, 1586w, 1492w, 1404m, 1281s, 1154w, 1132w, 1072m, 1005w, 908w, 830w, 797w, 740w, 674w, 641w, 557w, 424w.

Synthesis of $[(C_7H_6O_3)\cdot(C_8H_{12}N_2)_{1.5}]$ (8) The same procedure as that for **4** was used except for the introduction of 3-hydroxybenzoic acid (0.0276 g, 0.2 mmol) instead of 6-hydroxy-2-naphthoic acid. The resultant solution was left standing at room temperature for 2 weeks, colorless block crystals were obtained after slow evaporation of the solution. Yield: 85%. Anal. Calcd for $C_{19}H_{24}N_3O_3$ (%): C, 66.67; H, 7.02; N, 12.28. Found (%): C, 66.18; H, 7.55; N, 11.82. IR(cm^{-1}): 3093m, 2995m, 2949m, 2917m, 2824m, 2725m, 2696m, 2572m, 2523m, 2463m, 1961m, 1914m, 1799w, 1694s, 1620w, 1589s, 1480s, 1448s, 1413s, 1384m, 1359m, 1305m, 1282s, 1256s, 1227s, 1185m, 1097m, 1081w, 988s, 923s, 859w, 851w, 801w, 766s, 724w, 685m, 659m, 555w, 523w, 461w.

X-Ray crystallography

Compounds **1–8** were examined under a microscope and good-quality crystals were chosen for structure determination by X-ray diffraction using an optical microscope. Single-crystal X-ray diffraction measurements of the eight compounds were collected on a Siemens Smart CCD diffractometer at 293(2) K with MoKα radiation (λ = 0.71073 Å) by ω scan mode. There was no evidence of crystal decay during data collection. Semiempirical absorption corrections were applied using SADABS program, and the program SAINT was used for integration of the diffraction profiles[19]. All structures were solved by direct methods using the SHELXS and refined by full-matrix least-squares on F^2 with SHELXL program of the SHELXTL package[20]. All non-H atoms were refined anisotropically. Hydrogen atoms were first observed in difference E-maps and then placed in the calculated sites and included in the final refinement in the riding model approximation with fixed thermal factors. Further details for unit-cell parameters and structural refinement parameters are summarized in Table 1.

Table 1 Crystallographic Data and Structure Refinement Parameters for the Crystals of **1-8**

	1	**2**	**3**	**4**	**5**	**6**	**7**	**8**
Empirical formula	$C_{12}H_{18}NO_4$	$C_{33}H_{36}N_3O_{12}$	$C_{11}H_{13}N_2O_5$	$C_{30}H_{28}N_2O_6$	$C_{12}H_{13}N_2O_7$	$C_{16}H_{18}N_2O_4$	$C_{12}H_{12}N\ O_4$	$C_{19}H_{24}N_3O_3$
M	240.27	666.65	253.23	512.54	297.24	302.32	234.23	342.41
Crystal system	monoclinic	monoclinic	monoclinic	monoclinic	triclinic	triclinic	monoclinic	monoclinic
Space group	$P2_1/n$	$P2_1/c$	$P2_1/c$	$P2_1/c$	$P\bar{1}$	$P\bar{1}$	$P2_1/n$	$P2_1/c$
a/ Å	5.4960(9)	9.6944(4)	7.3345(7)	14.650(7)	7.8574(13)	7.5343(14)	7.4101(6)	9.3995(12)
b/Å	12.831(2)	17.9372(7)	10.9381(11)	12.512(6)	8.3711(11)	8.9454(17)	10.2133(9)	17.904(2)
c/Å	17.881(3)	18.6161(6)	15.0352(15)	14.649(7)	11.1437(13)	12.885(3)	15.0232(16)	11.3775(13)
α/deg	90	90	90	90	88.282(2)	99.769(4)	90	90
β/deg	93.872(3)	91.427(3)	92.804(2)	93.13	72.163(1)	103.689(4)	95.937(9)	93.243(2)
γ/deg	90	90	90	90	84.647(2)	108.465(3)	90	90
V/Å^3	1258.0(3)	3236.2(2)	1204.8(2)	2681(2)	694.70(17)	771.6(3)	1130.88(18)	1911.7(4)
Z	4	4	4	4	2	2	4	4
ρ_{calcd} (g/cm^3)	1.269	1.368	1.396	1.270	1.421	1.301	1.376	1.190
μ(mm^{-1})	0.095	0.105	0.112	0.127	0.119	0.094	0.104	0.082
F(000)	516	1404	532	1166	310	320	492	732
Total/independent	7893/3037	9481/5234	7473/2903	16329/6388	3459/3172	4994/3537	3956/2123	12163/4648
parameters	154	441	179	347	198	199	154	226
R_{int}	0.0572	0.0308	0.0982	0.0787	0.0591	0.0486	0.0126	0.0994
R^a, $R_w{}^b$	0.0791, 0.2435	0.0763, 0.2483	0.0597, 0.1768	0.0573, 0.2065	0.0612, 0.1872	0.0873, 0.2474	0.0527, 0.1161	0.0712, 0.2241
GOF on F^2	1.083	1.084	1.042	1.091	1.071	1.053	1.047	0.996

$^aR_1 = \Sigma||F_o|-|F_c||/\Sigma|F_o|$; $wR_2{}^b = \{\Sigma[w(F_o^2-F_c^2)^2]/\Sigma[w(F_o^2)]^2\}^{1/2}$

Results and discussion

Preparation of compounds 1-8

Both base and acid reagents have good solubility in water and common organic solvents, such as methanol, ethanol, acetone, N,N-

dimethylformamide and tetrahydrofuran except that 2,6-pyridinedicarboxylic acid needs to be dissolved in hot water or hot ethanol. Considering the number of hydrogen-bonding donor/acceptor groups in each component, crystallization of 2,3,5,6-tetramethylpyrazine with the acid blocks were carried out in different ratios. For compound **1**, **2**, **4**, **5,** **7** and **8**, 2,3,5,6-tetramethylpyrazine was directly mixed with a certain amount of acid-type reagents in ethanol/acetone and water solution, which were allowed to evaporate at room temperature to give the final crystalline products. In the case of **3** and **6**, acid and base were dissolved in different solvents individually and then mixed with each other to

Table 2 Hydrogen-Bond Geometries in the Crystal Structures of **1**-**8**

Compound	D–H···A (Å)	D–H (Å)	H···A (Å)	D···A (Å)	D–H···A (deg)	symmetry
1	O2–H2···O3	0.82	1.88	2.681	165	2.5-x, -0.5+y, 0.5-z
	O1–H1···N1	0.82	1.92	2.709	161	1+x, y, z
	C5–H5A···O4	0.98	2.75	3.630	149	-1+x, y, z
2	O11–H11···O8	0.82	1.81	2.574	153	1-x, 1.5+y, 0.5-z
	O7–H7···O5	0.82	1.83	2.555	147	1-x, 1.5+y, 0.5-z
	O8–H8···N2	0.82	1.84	2.651	173	-x, 0.5+y, 0.5-z
	O2–H2···O4	0.82	1.81	2.531	146	x, 1+y, 1+z
	O9–H9···O6	0.82	1.81	2.542	147	1-x, 2-y, 1-z
	O4–H4···O12	0.82	1.65	2.430	159	1-x, 2-y, 1-z
	O1–H1···O3	0.82	1.84	2.562	146	x, 1+y, 1+z
	N3–H3···O6	0.86	1.86	2.719	178	x, 1+y, 1+z
	O10–H10···O12	0.94	1.72	2.556	147	1-x, -0.5+y, 0.5-z
	O10–H10···O11	0.94	2.49	3.118	124	1-x, 1-y, -z
	C21–H21A···O9	0.93	2.61	3.382	141	-1-x, 1-y, 2-z
	C20–H20A···O10	0.93	2.64	3.421	142	-1-x, -y, -z
	C28–H28A···O9	0.93	2.53	3.453	169	1-x, 1-y, 1-z
	C24–H24C···O10	0.96	2.63	3.583	175	x, y, z
3	O3–H3···O1W	0.82	1.73	2.548	175	1+x, y, z
	O1W–H1WB···O1	0.94	1.89	2.825	173	1-x, 0.5+y, 0.5-z
	O4–H4···N2	0.82	1.91	2.696	160	x, -1+y, z
	O1W–H1WB···N1	0.94	2.49	2.951	110	1-x, 0.5+y, 0.5-z
	C5–H5A···O2	0.93	2.52	3.322	145	x, 0.5-y, -0.5+z
4	O4–H4···O1	0.84	1.86	2.700	173	-x, 1-y, -z
	O6–H6···O4	0.82	1.97	2.783	171	x, 0.5-y, 0.5+z
	O5–H5···N1	0.82	1.93	2.724	164	-x, 0.5+y, 0.5-z
	O3–H3···N2	0.82	1.98	2.800	175	1-x, 1-y, 1-z
	C26–H26A···O2	0.93	2.57	3.383	147	-1+x, y, z
	C23–H23A···O2	0.93	2.62	3.328	133	-x, -y, -z
	C14–H14A···O6	0.93	2.74	3.523	142	-1+x, y, 1+z
5	O3–H3···O1W	0.82	1.76	2.574	170	1-x, -y, 1-z
	O1W–H1WA···O1	0.79	1.95	2.738	178	1-x, 1-y, 1-z
	O1W–H1WB···O2	0.84	2.05	2.859	162	-1+x, y, z
	O4–H4···N1	0.82	1.82	2.638	172	1+x, y, z
	C2–H2C···O2	0.96	2.83	3.664	146	x, y, 1+z
	C2–H2A···O6	0.96	2.46	3.279	143	x, -1+y, z
6	O2–H2···N1	0.82	1.91	2.730	174	-1+x, y, z
	O3–H3···N2	0.82	1.92	2.703	159	-1+x, y, z
	C1–H1C···O1	0.96	2.55	3.345	140	1+x, y, z
	C9–H9A···O1	0.93	2.45	3.313	153	1+x, y, z
	C4–H4C···O2	0.96	2.69	3.553	150	1-x, -y, 1-z
	C13–H13A···O4	0.93	2.72	3.576	153	x, y, -1+z
7	O3–H3···O2	0.82	1.83	2.645	169	2-x, -y, -z
	O4–H4···N1	0.82	1.93	2.724	164	1+x, y, z
	C1–H1B···O1	0.95	2.68	3.412	134	0.5+x, 1.5-y, -0.5+z
	C10–H10A···O3	0.93	2.75	3.554	145	1.5+x, 0.5-y, -0.5+z
	C1–H1A···O1	0.96	2.82	3.615	141	2-x, 2-y, 2-z
8	O2–H2···N3	0.82	1.87	2.69	171	-1+x, 0.5-y, -0.5+z
	O3–H3···N2	0.82	1.96	2.77	167	x, 0.5-y, -0.5+z
	C8–H8A···O3	0.96	2.70	3.48	139	1-x, -y, -z
	C8–H8C···O2	0.96	2.73	3.58	150	1-x, 1-y, -z

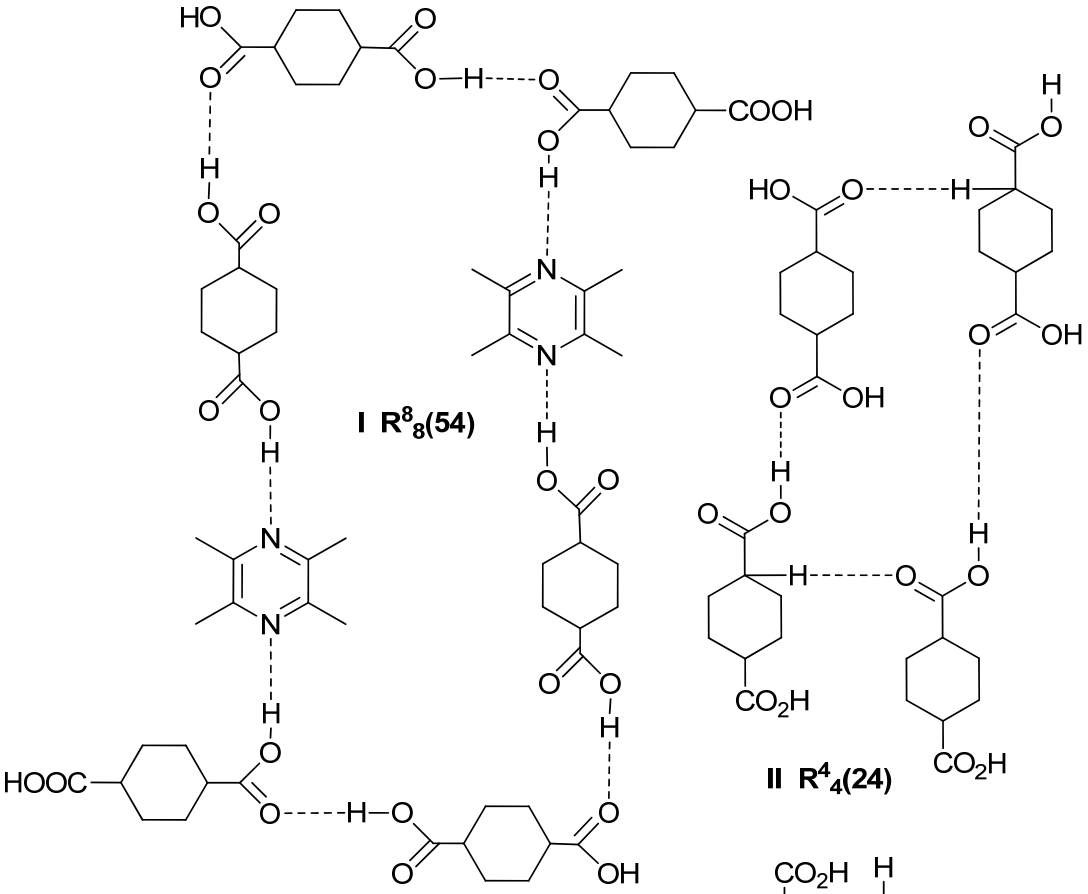

I $R^8_8(54)$

II $R^4_4(24)$

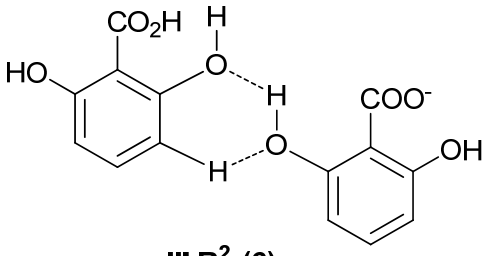

III $R^2_2(6)$

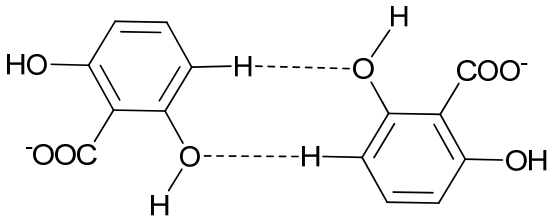

IV $R^2_2(8)$

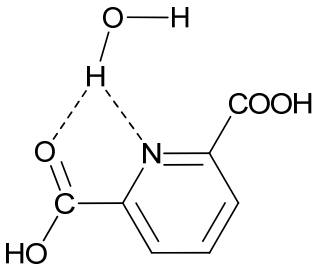

VI S(5)

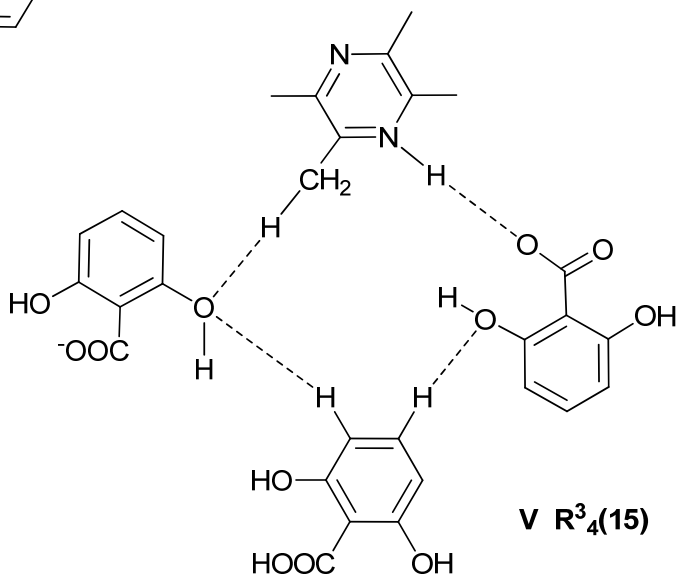

V $R^3_4(15)$

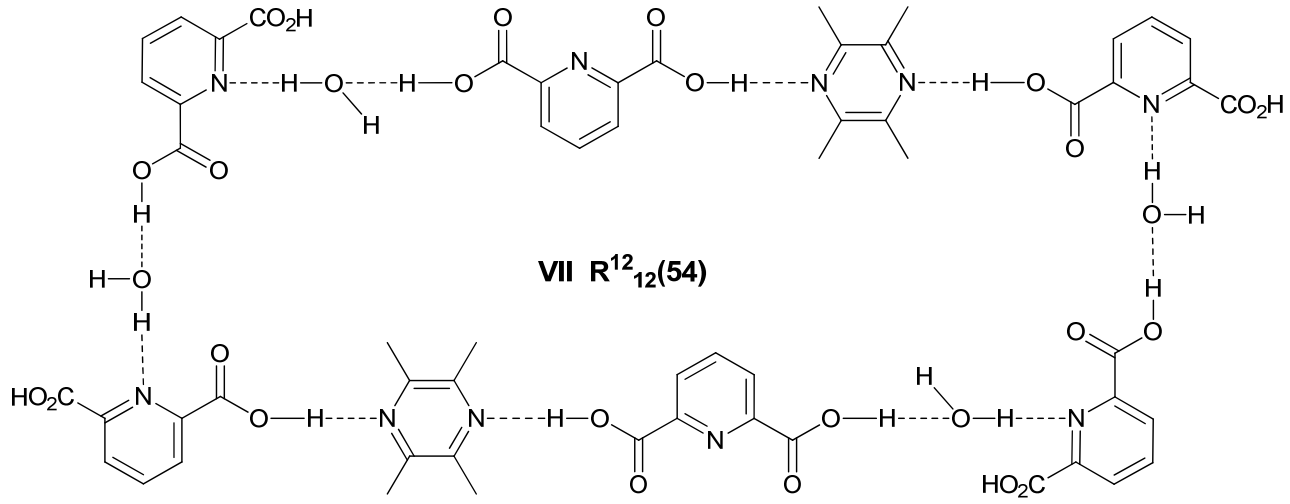

VII $R^{12}_{12}(54)$

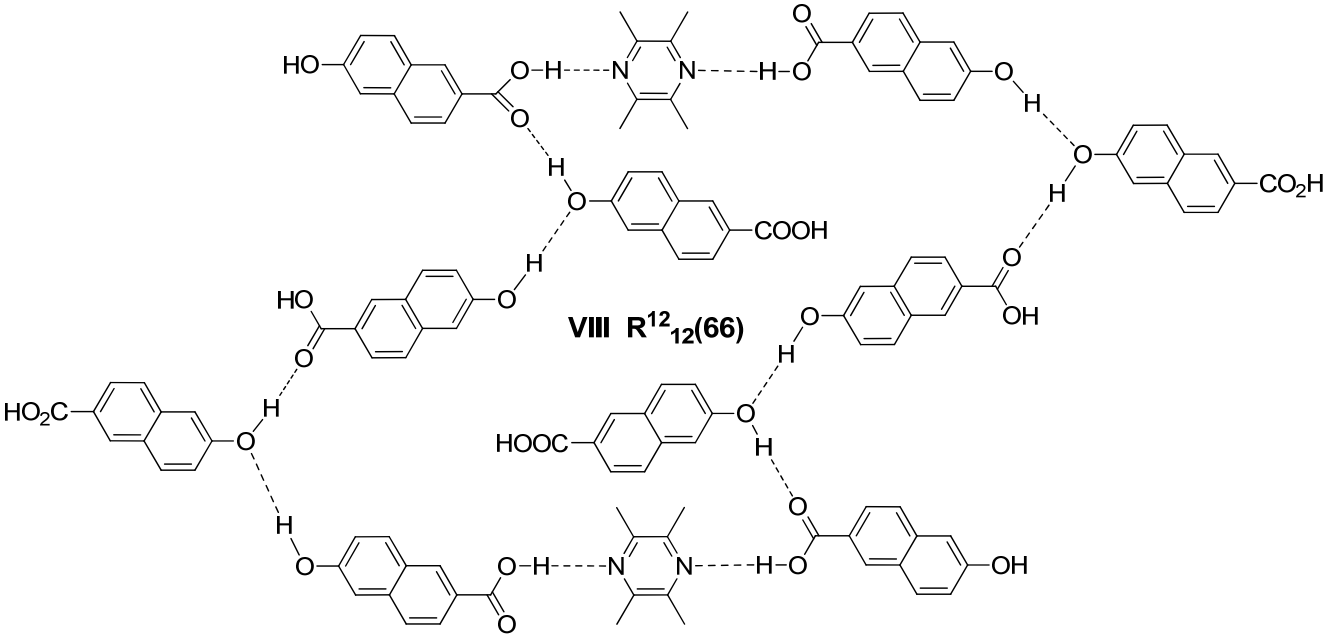

VIII $R^{12}_{12}(66)$

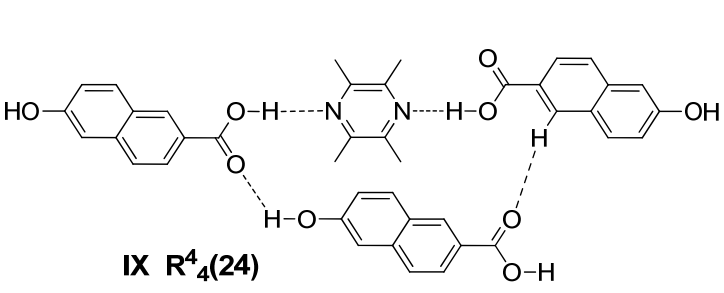

IX $R^{4}_{4}(24)$

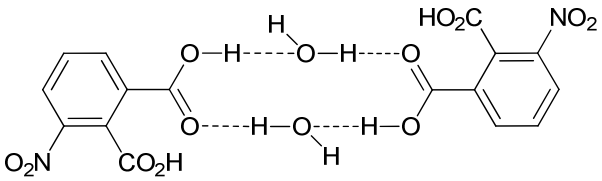

X $R^{4}_{4}(12)$

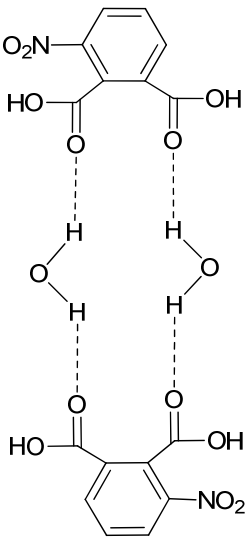

XI $R^{4}_{2}(18)$

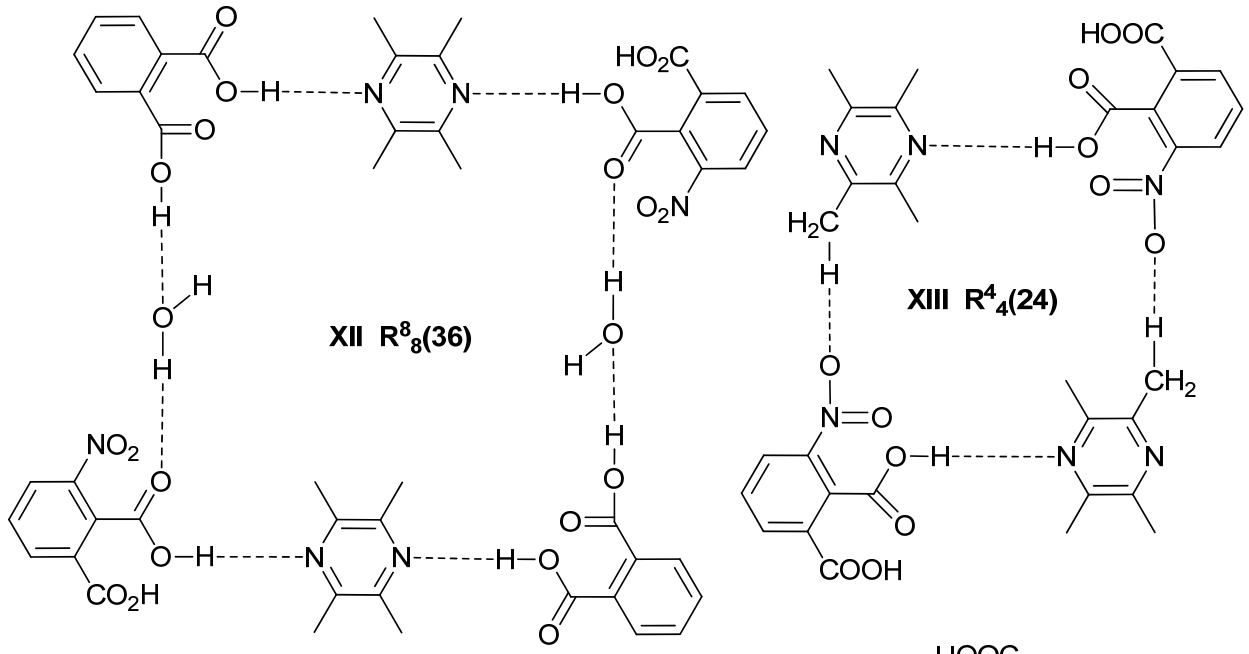

XII $R^8_8(36)$

XIII $R^4_4(24)$

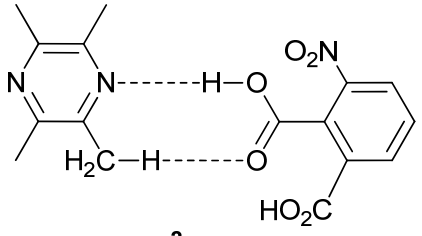

XIV $R^2_2(8)$

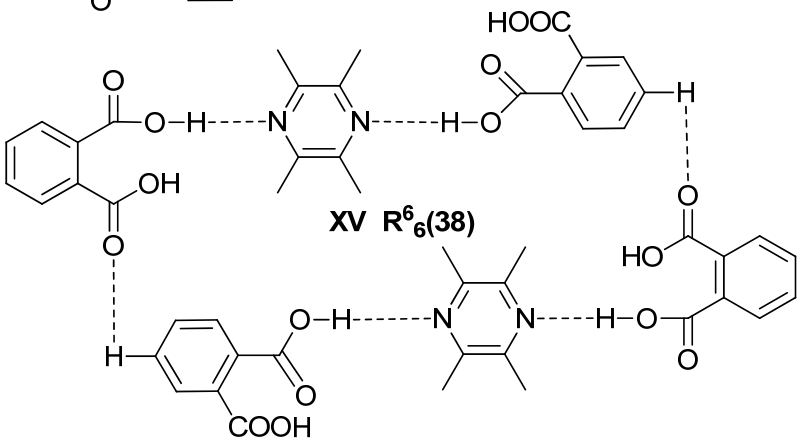

XV $R^6_6(38)$

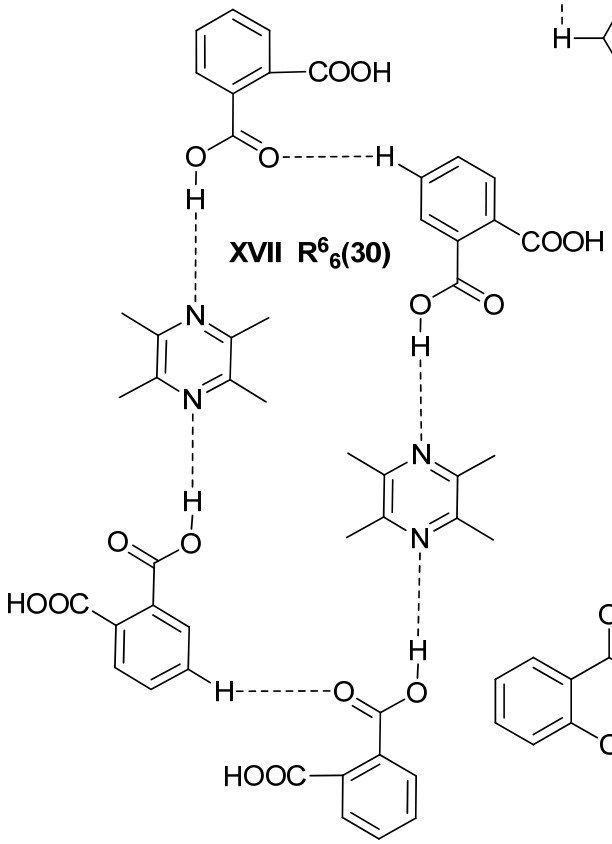

XVII $R^6_6(30)$

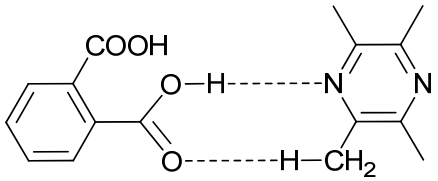

XVI $R^2_2(8)$

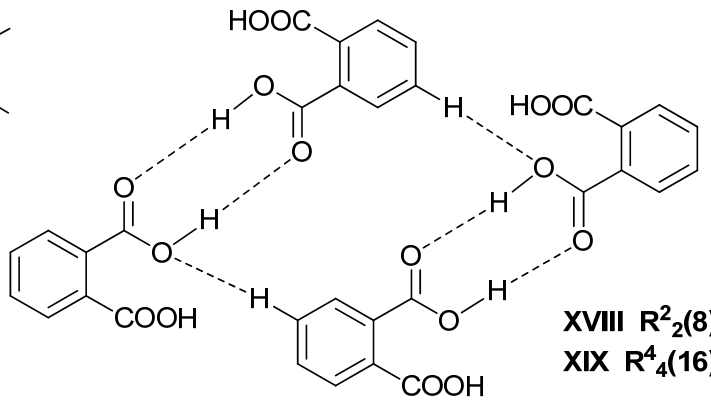

XVIII $R^2_2(8)$ &
XIX $R^4_4(16)$

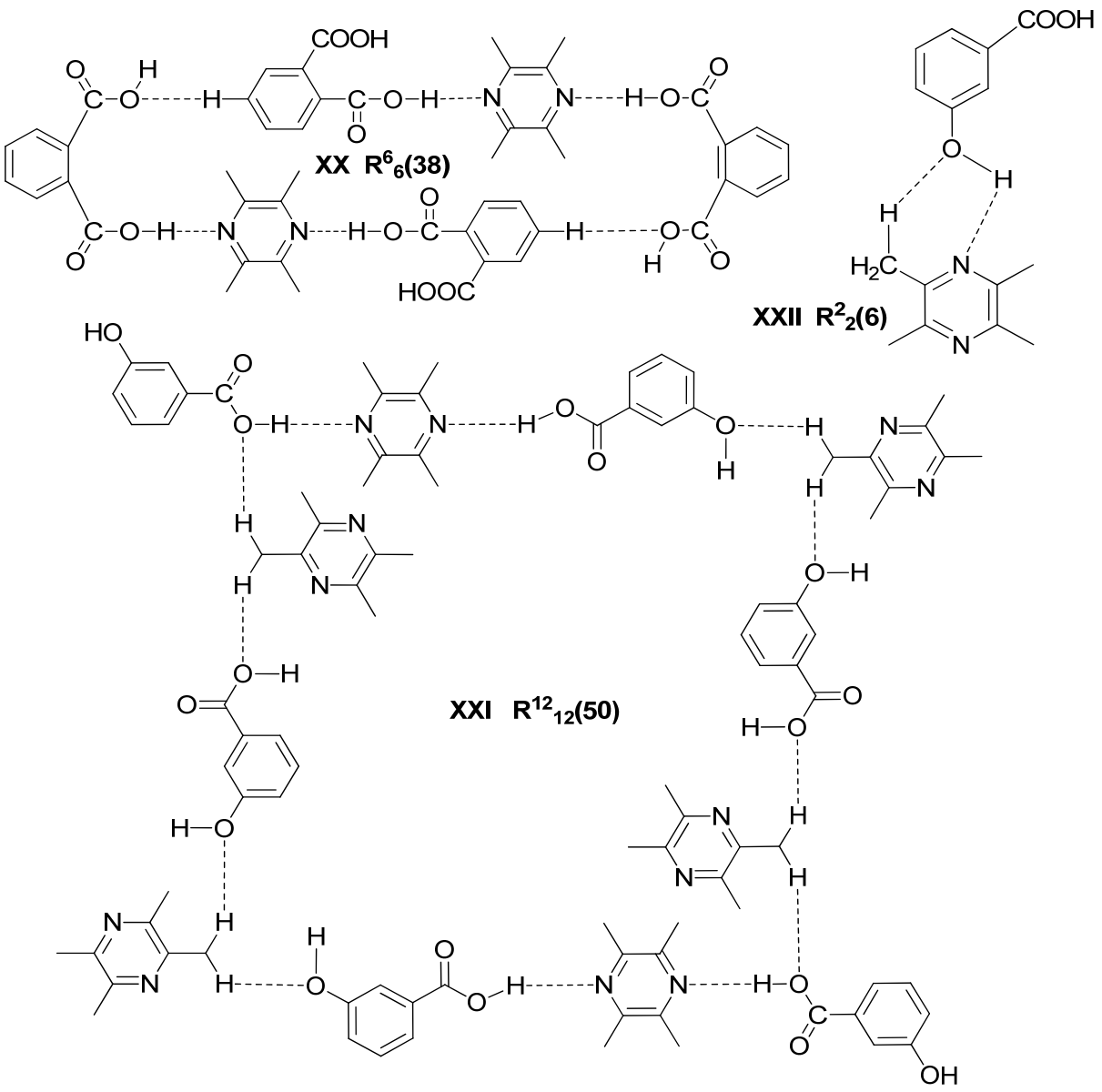

Scheme 2 Supramolecular synthons of **1-8 (**$R^a_d(n)$: "R" is the logogram of "ring"; "a" and "d" denote the numbers of acceptors and donors, respectively ; "n" denotes the number of atoms of the ring.**)**

obtain the single crystals suitable for X-ray determination. For compound **3**, base was dissolved in ethanol solvent and acid was dissolved in hot water. In the preparation of **6**, base was dissolved in tetrahydrofuran solvent and acid was dissolved in water. The schematic representations of related hydrogen-bonding synthons are summarized in Scheme 2. Hydrogen-bond parameters of compounds **1-8** are listed in Table 2.

Molecular and Supramolecular Structures of 1-8

Structure description of compound 1. The crystal structure of **1** consists of one 1,4-cyclohexanedicarboxylic acid molecule and a half 2,3,5,6-tetramethylpyrazine molecule and the crystal structure belongs to the monoclinic $P2_1/c$ space group (see Figure 1a). The 1,4-cyclohexanedicarboxylic acid molecule keeps the chair conformation. The dihedral angle formed between bond C5-C9 and the plane of C6/C5/C12 is 48.311(2)°. Similarly, the dihedral angle formed between bond C11-C7 and the plane of C8/C11/C10 is 73.298(8)°. First, 1,4-cyclohexanedicarboxylic acid molecules are connected together via strong hydrogen-bond O2(-COOH)-H2···O3(-COO2) to form a 1D helical chain along the crystallographic [001] direction (Figure 1b left). On this basis, the adjacent 1D helical chains are linked by 2,3,5,6-tetramethylpyrazine molecules to generate 2D supramolecular sheet via strong hydrogen-bond O1(-COOH)-H1···N1 along the crystallographic [100] direction (Figure 1b right), containing a big synthon I $R^8_8(54)$. Further analysis of the crystal packing indicated that the interlayered weak hydrogen-bonds C5-H5A···O4(-COOH) link two adjoining parallel sheets to give a 3D supramolecular network, with synthon II $R^4_4(24)$ can be found (Figure 1d).

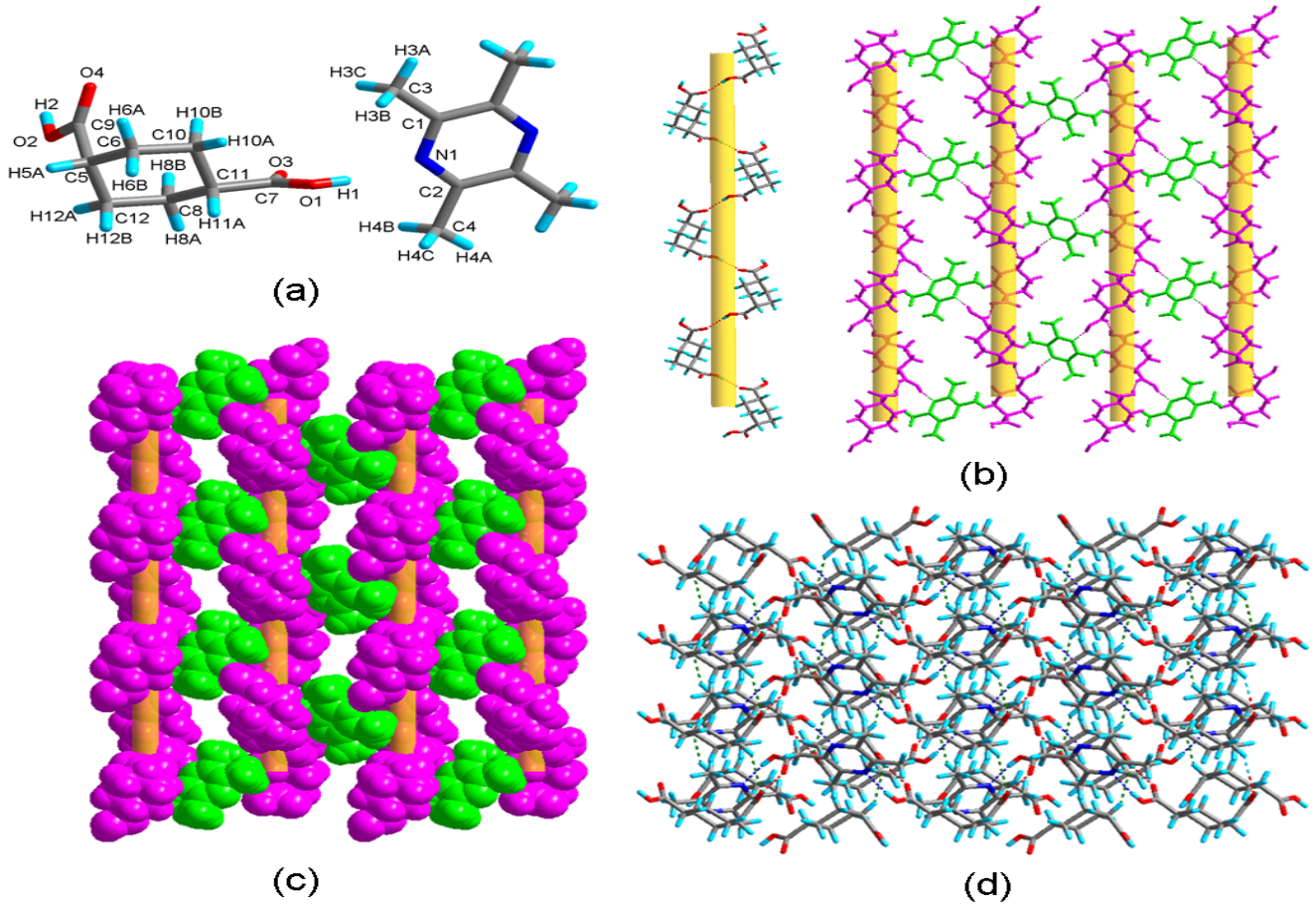

Fig. 1 (a) Molecular structure of **1** with atom labeling of the asymmetric unit. (b) 1D infinite helical chain (left) and 2D network consisting of helix units (right). (c) Space-filling model of the 2D network. (d) 3D supramolecular architecture along the [001] direction. (O, red; N, blue; C, gray; H, turquoise in this and the subsequent figures)

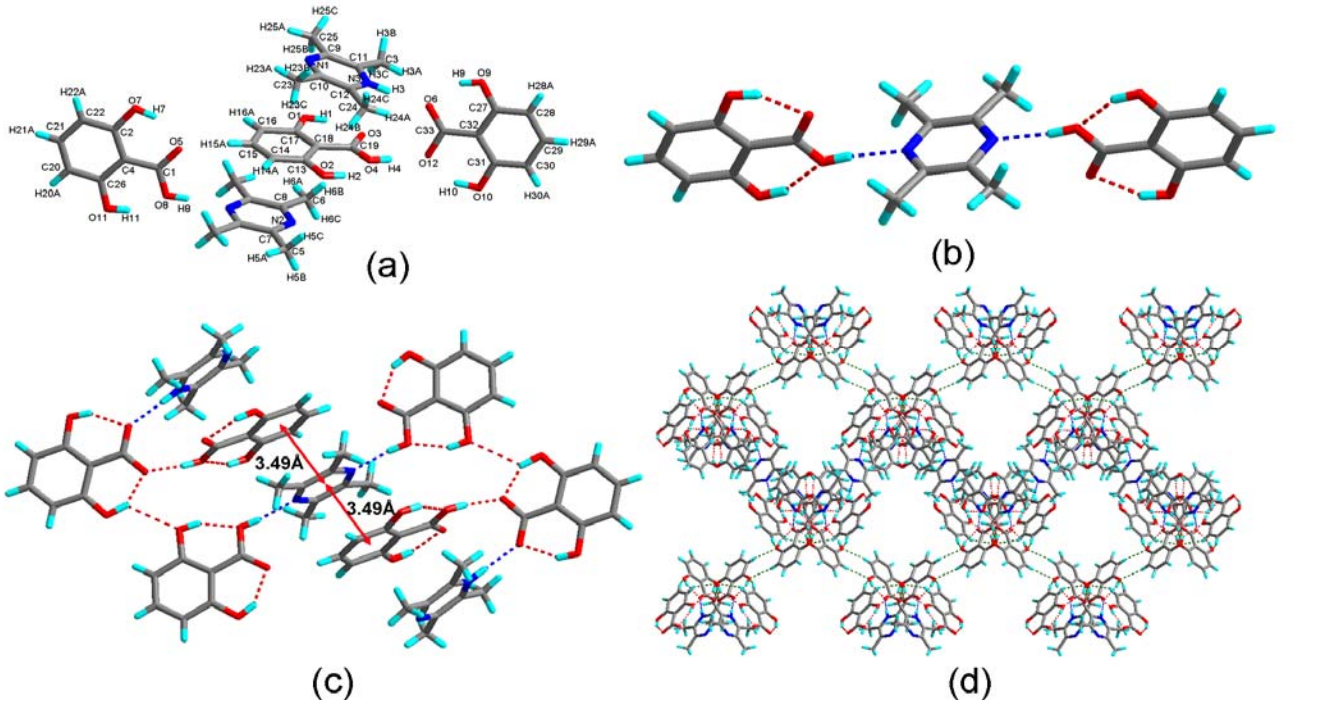

Fig. 2 (a) Molecular structure of **2** with atom labeling of the asymmetric unit. (b) Tripolymer motif assembled via O-H···N. (c) Multimer motif assembled via H-bonds and π-π interactions. (d) 3D supramolecular architecture along the [001] direction.

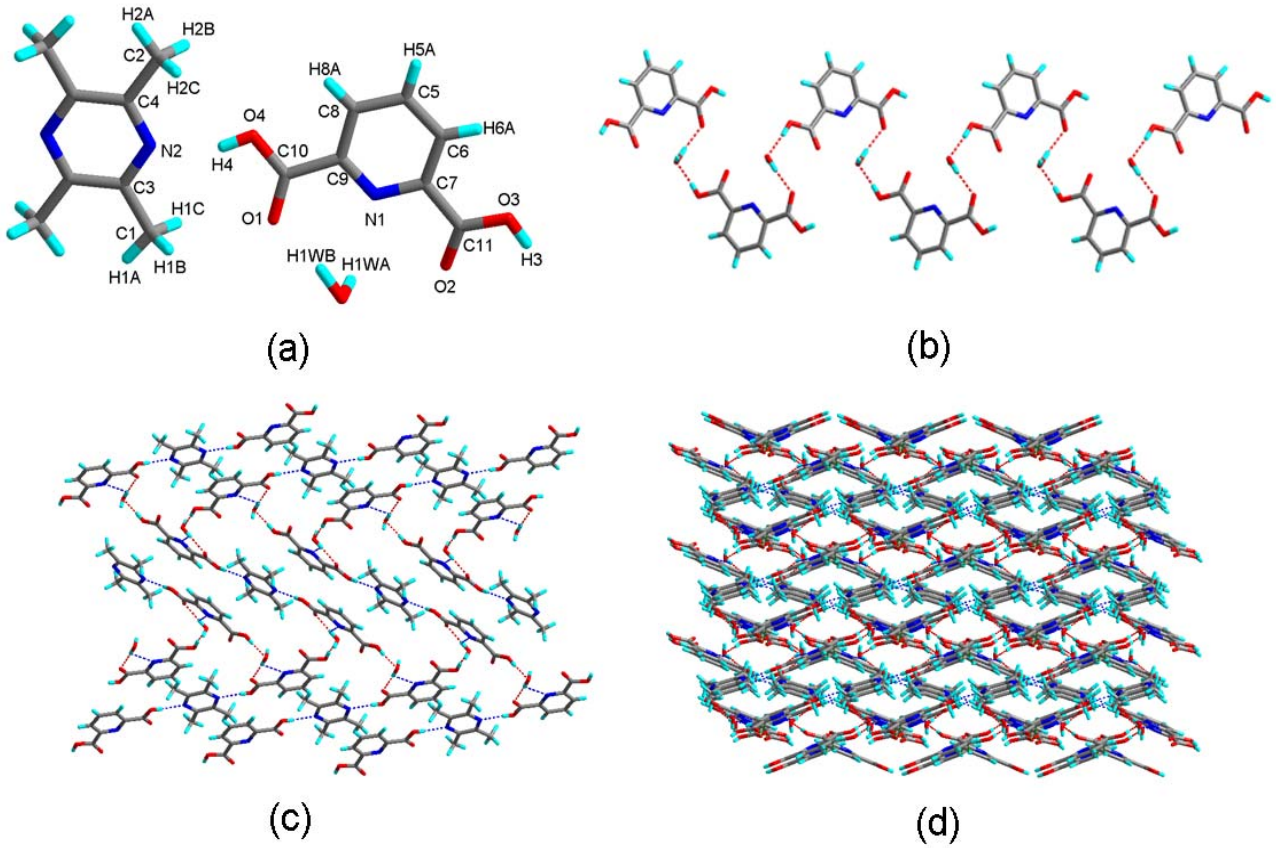

Fig. 3 (a) Molecular structure of **3** with atom labeling of the asymmetric unit. (b) 1D double chain along the [100] direction. (c) A side view of 2D wavelike supramolecular sheet. (d) 3D supramolecular network along the crystallographic [001] direction.

Structure description of compound 2. As depicted in Figure 2a, proton-transfer organic salt **2** crystallized with two 2,6-dihydroxybenzoic acid molecules, one 2,6-dihydroxybenzoic acid monoanion, a half 2,3,5,6-tetramethylpyrazine molecule and one 2,3,5,6-tetramethylpyrazine monocation in the asymmetric unit. The crystal structure belongs to the monoclinic $P2_1/c$ space group. First, 2,3,5,6-tetramethylpyrazine molecule links two 2,6-dihydroxybenzoic acid molecules to generate a centrosymmetric tripolymer motif via O8(-COOH)-H8···N2 bonds, with O7(-OH)-H7···O5(-COOH) and O11(-OH)-H11···O8 (-COOH) intramolecular interactions of 2,6-dihydroxybenzoic acid molecules (Figure 2b). Afterwards, there exists intermolecular interactions O10(-OH)-H10···O11(-OH), N3-H3···O6(-COO^-) and O4(-OH)-H4…O12(-COO^-) which extend a tripolymer to afford a centrosymmetric multimer motif, meanwhile, several strong intramolecular interactions of 2,6-dihydroxybenzoic acid molecule/monoanion (O10(-OH)-H10···O12(-COO^-), O9(-OH)-H9···O6(-COO^-), O2(-OH)-H2···O4(-COOH) and O1(-OH)-H1···O3(-COOH)) also can be found. Therein, the phenomena of π-π stacking can be seen, where the distances between pyrazine ring and the neighbouring aryl rings are 3.49Å. The dihedral angle between the plane of C13-C18 aryl ring of the acid molecule and the plane consisting of atoms C7/C8/N1/N2 of the base component is 1.04°, which are nearly parallel and with the formation of synthon III $R^2_2(6)$, as is shown in Figure 2c. Furthermore, the quite fascinating three-dimensional arrangement is created due to the presence of a series of weak hydrogen-bonds, that is C21-H21A···O9(-OH), C20-H20A···O10(-OH), C28-H28A···O9(-OH) and C24-H24C···O10(-OH) (synthon IV $R^2_2(8)$ and V $R^3_4(15)$) (Figure 2d).

Structure description of compound 3. In the local structure of cocrystal **3** as shown in Figure 3a, the molecular structure of **3** contains one 2,6-dihydroxybenzoic acid molecule, a half 2,3,5,6-tetramethylpyrazine molecule and a water solvate in the monoclinic $P2_1/c$ space group. The dihedral angle between the plane of pyrazine ring and the plane of carboxyl functional groups C10/O1/O4 and C11/O2/O3 are 6.589(1)° and 10.216(2)° respectively. Each lattice water acts as a hydrogen-bonding connector, joining 2,6-dihydroxybenzoic acid subunits to generate 1D double chain via strong O3(-COOH)-H3···O1W and O1W-H1WB···O1(-COOH) bonds along the [100] direction (see Figure 3b). Moreover, hydrogen bonds O4(-COOH)-H4···N2 and O1W-H1WB···N1 extend the acid -base subunits to form a unique 2D wavelike supramolecular sheet, containing synthons VI S(5) and VII $R^{12}_{12}(54)$, as shown in Figure 3c. There exist interlayer C5-H5A···O2 hydrogen-bonding interactions between C5 donors and O2 acceptors of 2,6-dihydroxybenzoic acid molecules, which connect the adjoining parallel sheets to general a 3-D supramolecular network along the crystallographic [001] direction (see Figure 3d).

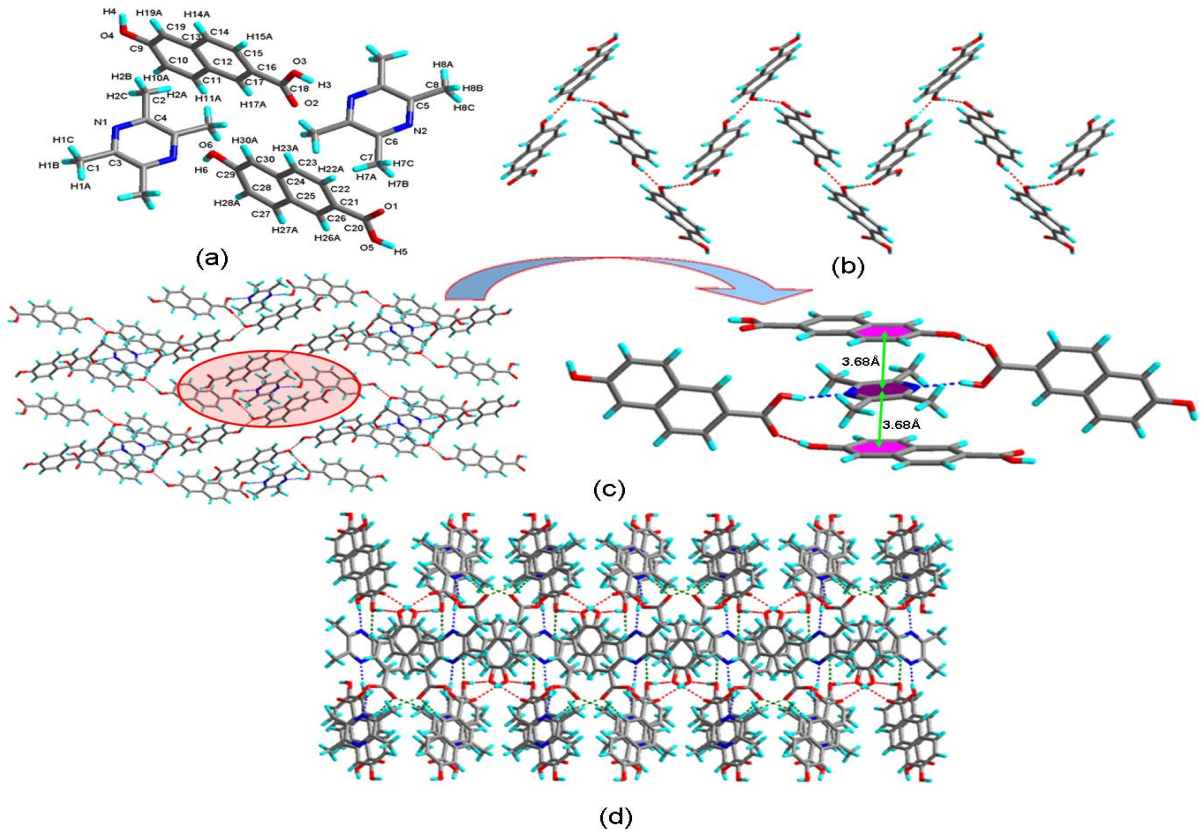

Fig. 4 (a) Molecular structure of **4** with atom labeling of the asymmetric unit. (b) 1D zigzag-chain along the [100] direction. (c) 2D networks along the crystallographic [001] direction (left) and π-π stacking phenomenon (right). (d) 3D supramolecular architecture along the crystallographic [001] direction.

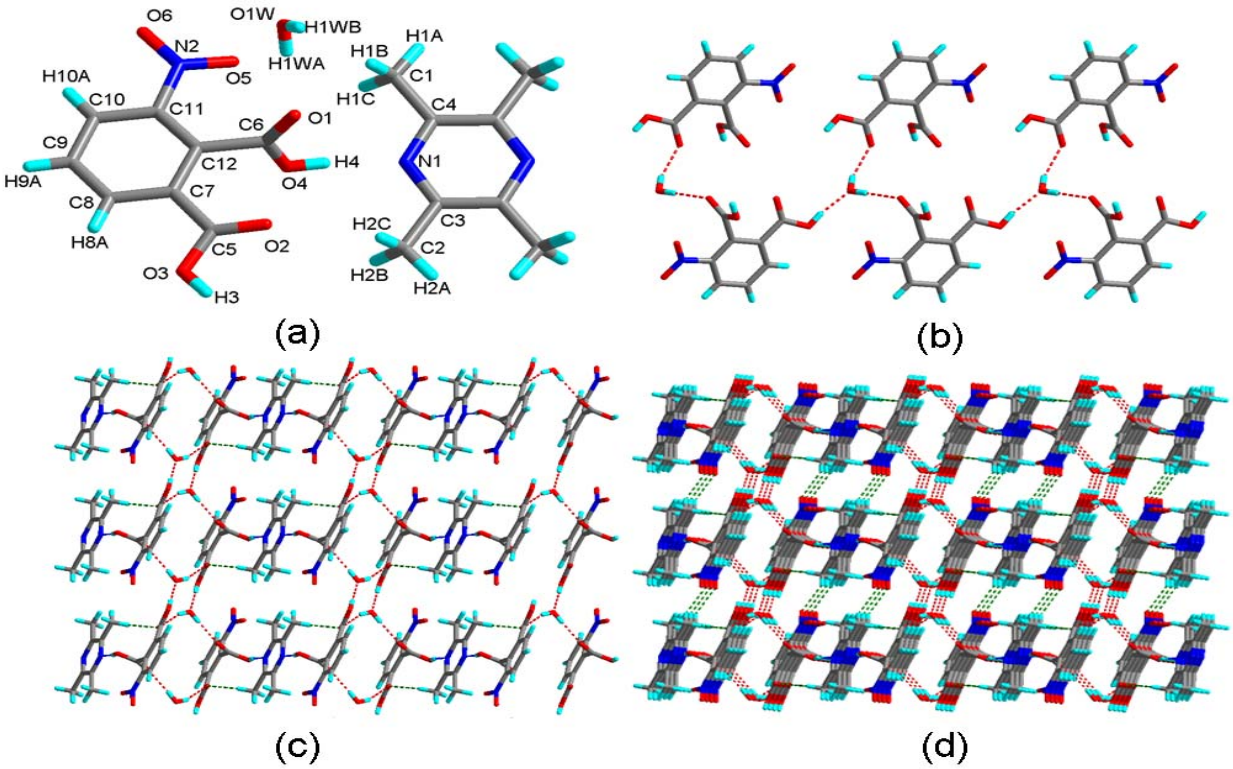

Fig. 5 (a) Molecular structure of **5** with atom labeling of the asymmetric unit. (b) 1D tape-chain along the crystallographic [001] direction. (c) Two-dimension network along the crystallographic [100] direction. (d) 3D supramolecular sheets along the crystallographic [100] direction.

Structure description of compound 4. In the molecular structure of **4**, there exists two 6-hydroxy-2-naphthoic acid molecules and two halfs 2,3,5,6-tetramethylpyrazine molecules in the monoclinic $P2_1/c$ space group as shown in Figure 4a. Within 6-hydroxy-2-naphthoic acid molecules, the carboxyls make dihedral angles of 6.736(2)° and 6.187(2)° respectively with the naphthalene rings, and the dihedral angle between the two naphthalene rings is 5.989(5)°. The adjacent acid components are linked by O6(-OH)-H6···O4(-COOH) and O4(-COOH)-H4···O1(-OH) to form a wide tape along the crystallographic [100] direction (Figure 4b). Hydrogen-bonding O5(-COOH)-H5···N1 connect 1D zigzag-chains to form 2D networks along the crystallographic [001] direction (Figure 4c). Furthermore, there exists an interlayered hydrogen-bonding O3(-COOH)-H3···N2 (synthon VIII, $R^{12}_{12}(66)$), which extends the adjoining parallel sheets to afford a 3-D array (Figure 4d). At the same time, the crystal packing consists of face-to-face π-π stacking between pyrazine ring and aryl ring (centroid-centroid distances=3.68 Å), which is also an interchain interaction. And weak hydrogen-bonding interactions C14-H14A···O6, C23-H23A···O2 and C26-H26A···O2 further consolidating this 3-D structure along the crystallographic [001] direction, containing synthon IX $R^4_4(24)$.

Structure description of compound 5. As depicted in Figure 5a, the molecular structure of **5** which belongs to the triclinic $P\bar{1}$ space group, crystallizes with a 3-nitrophthalic acid molecule, a half 2,3,5,6-tetramethylpyrazine molecule and a water solvate. The C12-C6 and C7-C5 bonds distances of the carboxylic moiety are 1.516(22) Å and 1.501(24) Å, respectively, for 3-nitrophthalic acid molecule, significantly longer than the cyclic C-C bonds (average 1.388Å). Within 3-nitrophthalic acid subunit, two carboxyls form the dihedral angles of 81.529(9)° and 10.629(2)° respectively, with the plane of benzene ring. Oxygen atoms of water molecules act as hydrogen bond donors and acceptors, connecting 3-nitrophthalic acid molecules to form tape-chains along the crystallographic [001] direction by O3(-COOH)-H3···O1W, O1W-H1WB···O2(-COOH) and O1W-H1WA···O1(-COOH) (Figure 5b), and these tapes are further assembled via hydrogen-bonding O4(-COOH)-H4···N1 and C2-H2C···O2(-COOH) into a two-dimension network along the crystallographic [100] direction which containing synthons X $R^4_4(12)$, XI $R^4_2(18)$ and XII $R^8_8(36)$, as is shown in Figure 5c. The adjacent layers are connected via interlayered sustained interactions C2-H2A···O6(-NO_2) forming 3D supramolecular sheets along the crystallographic [100] direction (synthon XIII $R^4_4(24)$ and XIV $R^2_2(8)$) (Figure 5d). In previous work, Deng's group reported a supramolecular organic salt based on the same acid and piperazine assembled via hydrogen bonding[21]. In this compound, 3-nitrophthalic acid is diprotonated and piperazine is protonated. Compared with it, compound **5** is a cocrystal demonstrating that 2,3,5,6-tetramethylpyrazine has a tendency to form supramolecular cocrystal with acidic molecules.

Structure description of compound 6. In the crystal structure of **6**, the asymmetric unit consists of two halfs 2,3,5,6-tetramethylpyrazine molecules and one o-phthalic acid molecule belonging to the triclinic $P\bar{1}$ space group (Figure 6a). The dihedral angles between the aryl ring plane and two carboxyl rings (C16/O3/O4 and C15/O1/O2) are 57.0 and 29.7° respectively. The exocyclic bond C11-C15 and C12-C16 are elongated to 1.496(31) Å and 1.499(31) Å, respectively, longer than cyclic C-C bonds (average 1.384Å). Within o-phthalic acid molecule, the dihedral angles between two planes of carboxyls and the plane of benzene ring are 56.959(9)° and 29.684(1)° respectively. The adjacent acid and base components are linked via O2(-COOH)-H2···N1 and O3(-COOH)-H3···N2 to form a zigzag tape along the crystallographic [010] direction as is shown in Figure 6b. The 1D zigzag chains are connected into a 2D wavelike sheet along the crystallographic [010] direction through C1-H1C···O1(-COOH) and C9-H9A···O1(-

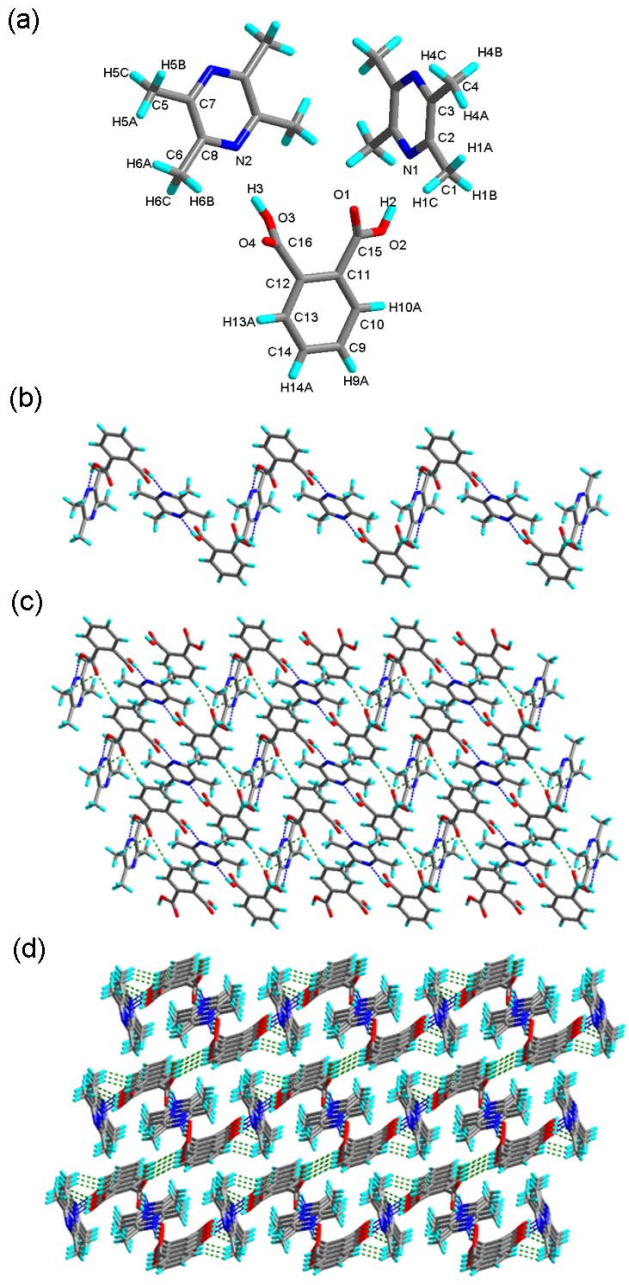

Fig. 6 (a) Molecular structure of **6** with atom labeling of the asymmetric unit. (b) 1D zigzag chain along the crystallographic [010] direction. (c) 2D wavelike sheet along the crystallographic [010] direction. (d) 3D supramolecular structure along the crystallographic [100] direction.

COOH) interactions (synthon XV $R^6_6(38)$ and XVI $R^2_2(8)$), as is shown in Figure 6c. Further analysis of the crystal packing suggests that C4-H4C···O2(-COOH) and C13-H13A···O4(-COOH) stabilize the three-dimensional supramolecular structure along the crystallographic [100] direction (Figure 6d), synthon XVII $R^6_6(30)$ can be found.

Structure description of compound 7. Cocrystal **7** consists of a half 2,3,5,6-tetramethylpyrazine molecule and one o-phthalic acid molecule in the monoclinic space group $P2_1/c$ (Figure 7a). Similarly to cocrystal **6,** the exocyclic bond C5-C7 and C6-C12 are elongated to 1.503(31) Å and 1.492(31) Å, respectively, longer than cyclic C-C bonds (average 1.388Å). In addition, the dihedral angles between two planes of carboxyls and the plane of benzene ring are 45.736(100)° and 45.596(147)° respectively. As illustrated in Figure 7b, each 2,3,5,6-tetramethylpyrazine molecule connects neighboring o-phthalic acid molecules via supramolecular homosynthon XVIII $R^2_2(8)$ and hydrogen bond O3(-COOH)-H3···N1 forming 1D zigzag chain along the crystallographic [001] direction. Adjacent parallel chains are arranged into 2D network along the crystallographic [001] direction through C1-H1B···O1(-COOH) and C10-H10A···O3(-COOH) (synthon XIX $R^4_4(16)$ and synthon XVI $R^2_2(8)$ (Figure 7c). Furthermore, weak hydrogen bonds C1-H1A···O1(-COOH) extend 2D networks to generate 3D supramolecular sheets along the crystallographic [100] direction, with synthon XX $R^6_6(38)$ can be found (Figure 7d).

It is to be noted that both compounds **6** and **7** are 3D supramolecular cocrystals constructed by o-phthalic acid and 2,3,5,6-tetramethylpyrazine, while the compound based on the same acid and *N,N'*-dimethylpiperazine in our previous work is a 2D supramolecular organic salt with H atom of o-phthalic acid transferring to the *N,N'*-dimethylpiperazine[15g]. This reveals that 2,3,5,6-tetramethylpyrazine is more likely to build cocrystal than *N,N'*-dimethylpiperazine.

Structure description of compound 8. Although the structure of compound **8** has been reported[14c], but studies of its structure in details have not been well explored. X-ray structural analysis of **8** reveals the asymmetric unit (Figure 8a) is composed of one 3-hydroxybenzoic acid molecule, one and a half 2,3,5,6-tetramethylpyrazine molecules in the monoclinic space group $P2_1/c$. The exocyclic bond C14-C13 is elongated to 1.486(28) Å, longer than cyclic C-C bonds (average 1.3814Å). The dihedral angle between the plane of C14-C15 aryl ring of the acid molecule and the plane consisting of atoms C9/C10/C11/C12 of the base component is 63.118°. As is shown in Figure 8b, strong hydrogen-bonds O2(-COOH)-H2···N3 and O3(-OH)-H3···N2 connect 3-hydroxybenzoic acid molecules and adjacent 2,3,5,6-tetramethylpyrazine molecules to form an infinite 1D linear chain along the crystallographic [001] direction. Furthermore, the 1D chains are interlinked by week hydrogen-bonds C8-H8A···O3(-OH) and C8-H8C···O2(-COOH), constituting cross-linked 2D networks

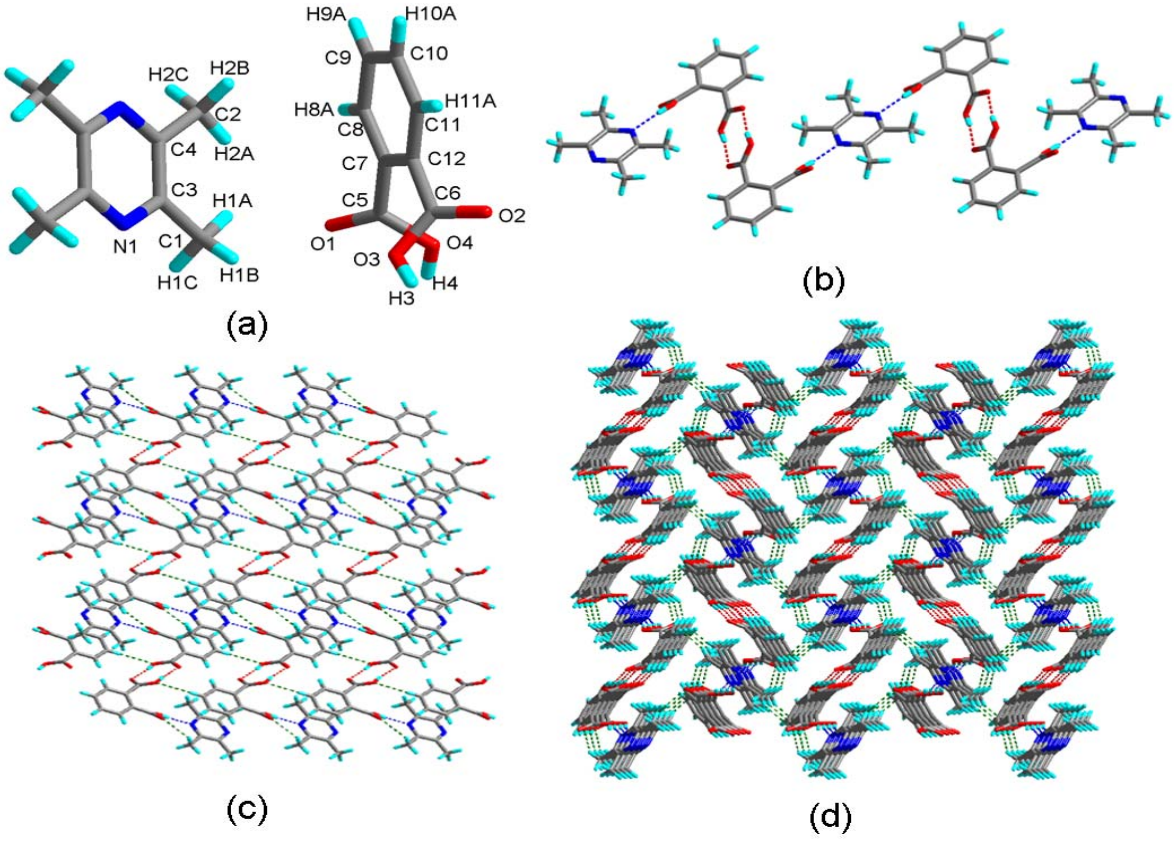

Fig.7 (a) Molecular structure of **7** with atom labeling of the asymmetric unit. (b) 1D zigzag chain along the crystallographic [001] direction. (c) 2D network along the crystallographic [001] direction. (d) 3D supramolecular sheet along the crystallographic [100] direction.

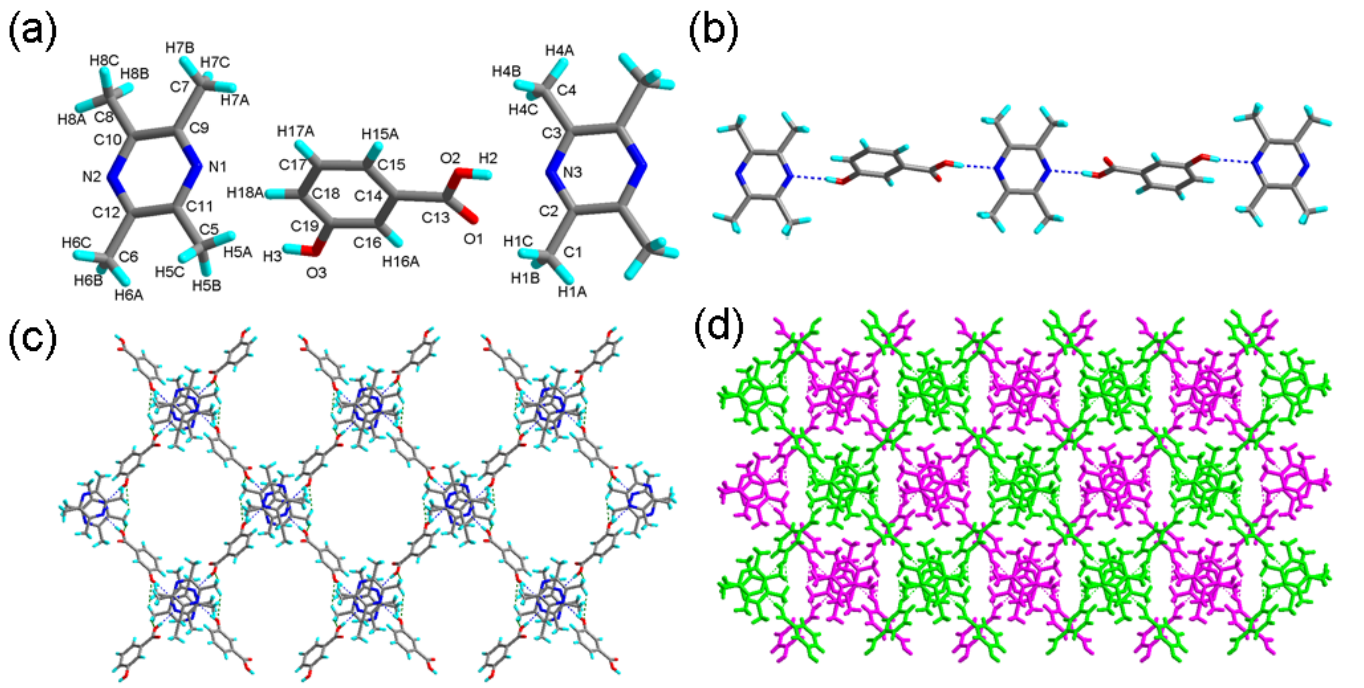

Fig. 8 (a) Molecular structure of **8** with atom labeling of the asymmetric unit. (b) 1D infinite chain along the [001] direction. (c) 2D network noticed the square cavities along the [001] direction. (d) The cavities are filled by adjacent layers due to offset packing.

along the crystallographic c direction (see Figure 8c), containing synthons XXI $R^{12}_{12}(50)$ and XXII $R^{2}_{2}(6)$. Layers stack with an offset in the adjacent layers (Figure 8d), so the formation of continuous channels are avoided, and no interlayer interactions such as hydrogen bonding or π-π stacking are observed.

Thermogravimetric Analysis

All compounds are air stable and can retain their structural integrity at ambient conditions for a considerable length of time. TGA was implemented to determine the thermal stability of these co-crystalline materials and the TGA curves are shown in Fig. 9. As for **1**, **2** and **8**, the TGA results indicate that they remain intact until 180°C, 120°C and 100°C, respectively, and then there is a sharp weight loss ending at 320°C for **1,** 270°C for **2** and 250°C for **8**, (peaks: 297°C for **1** 198°C for **2** and 167°C for **8**), corresponding to the explosion of all base and acid components. TGA curves of **3**, **4** and **5** show two consecutive weight losses of all crystalline samples from 55°C to 315°C (peaking at 104°C and 265°C, respectively), from 60°C to 330°C (peaking at 174°C and 277°C respectively), and from 70°C to 270°C (peaking at 194°C and 207°C, respectively), respectively. For example, the TGA curve of **3** displays a weight loss from 55°C to 112°C (found: 32.51%), which is attributed to the loss of the lattice water and base molecules (calcd: 33.99%). The residual host framework stays intact until 180°C, and there is a sharp weight loss peaking at 265°C and ending at 315°C, corresponding to the expulsion of all acid components. As for **6**, the TGA result indicates that it remains intact until 85°C, and then there is a sharp weight loss ending at 240°C (peaks: 190°C), corresponding to the loss of all base and acid components. For compound **7,** the TGA curves reveals a slow weight loss ending at 210°C (found: 29.06%), corresponding to the loss of acid component (calcd: 28.43%), and a sharp weight loss ending at 240°C (peaks: 212°C), corresponding to the loss of base component.

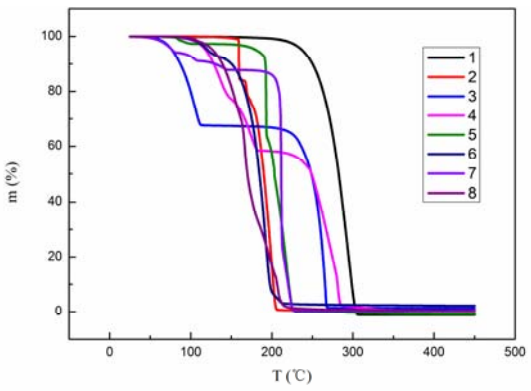

Figure 9. Thermogravimetric analysis for compounds **1-8**

Conclusions and perspectives

To design and predict the structures and properties of various crystalline materials is one of the ultimate goal of crystal engineering[22]. In the present work, 2,3,5,6-tetramethylpyrazine was introduced as supramolecular building block to construct crystalline materials which was demonstrated to have the tendency to build 3D supramolecular cocrystals. It is evident

that the N atom of the pyrazine ring can act as hydrogen-bonding donors/acceptors to fulfill the diversiform motives and the C atom of the four methyl-arms as potential hydrogen-bond donors to enrich the formation of homo- or heterosynthons.

In summary, the strong O-H···O and O-H···N hydrogen bonds play the main role in controlling the 1-D chains which is generally predictable. In addition, weak C-H···O hydrogen bonds are less robust but readily contribute to crystalline stabilization in all complexes. In all 2D/3D supramolecular compounds are fully appreciated the presence of weak C-H···O hydrogen bonds. They not only extend these networks from 1D to 2D or 2D to 3D, but also reinforce their structures because these synthons formed by C-H···O hydrogen bonds are stable in compounds 1-8. Whereas, the weak C-H···O interaction can affect crystal packing in unpredictable ways, so it need to be considered carefully in crystal engineering as addressed in Desiraju's recent account[23]. The absence of classical synthons $R^2_2(6)$ or $R^2_2(8)$ in compounds **1-4** which were usually observed in organic cocrystals of carboxylic acid and heterocyclic base may due to the stereochemistry effect. Moreover, plenty of big synthons exist in this study, such as synthons I, VII, VIII, XII, XIII, XV, XVII, XX and XXI. Clearly, containing 2,3,5,6-tetramethylpyrazine molecules is a common structural feature of these big synthons, despite C−H donors of methyls didn't participate in synthon formation in I, VII, VIII and XII. Moreover, their reproducibility and the ability to be predicted may be lower than the classical synthons, such as $R^2_2(8)$, in consideration of their volumes and complicated properties. Nevertheless, it is obvious that such building blocks will be frequently applied in developing their applications in the crystal engineering. Besides, we hope that the reliable "supramolecular synthon" strategy can be used for the design of novel periodic and predictable superstructures, and it may help in the design of new functional crystalline solids.

Acknowledgements

This work was supported by the National Natural Science Foundation of China (No. 51372125and 21203106), and the Natural Science Foundation of Shandong Province, China (No. ZR2011BL015).

Notes and references

1 (a) J. L. S. Rowsell, E. C. Spencer, J. Eckert, J. A. K. Howard; O. M. Yaghi, *Science*, 2005, **309**, 1350-1354; (b) P. K. Thallapally, T. B. Wirsig, L. J. Barbour, J. L. Atwood, *Chem. Commun.,* 2005, **35**, 4420-4422; (c) Y. He, S. Xiang and B. Chen, *J. Am. Chem. Soc*., 2011, 133, 14570-14573; (d) P. Li, Y. He, J. Guang, L. Weng, John C. G. Zhao, S. Xiang and B. Chen, *J. Am. Chem. Soc*., 2014, 136, 547-549; (e) J. Tian, P. K. Thallapally and B P. McGrail, *CrystEngComm*, 2012, 14, 1909-1919.

2 (a) J. R. G. Sander, Dejan-Krešimir Bučar, R. F. Henry, B. N. Giangiorgi, G. G. Z. Zhang and L. R. MacGillivray, *CrystEngComm*, 2013, **15**, 4816-4822; (b) B. Das and J. B. Baruah, *Cryst. Growth Des.*, 2011, **11,** 5522 – 5532.

3 (a) B. Nath and J. B. Baruah, *Cryst. Growth Des.*, 2013, **13,** 5146-5155; (b) R. Banerjee, P. M. Bhatt and G. R. Desiraju, *Cryst. Growth Des.*, 2006, **6,** 1468-1478; (c) D. Singh, P. K. Bhattacharyya and J. B. Baruah, *Cryst. Growth Des.*, 2010, **10,** 348-356; (d) S. Aitipamula, P. S. Chow and R. B. H. Tan, *CrystEngComm*, 2012, **14**, 691 – 699; (e) T. Hosokawa, S. Datta, A. R. Sheth, N. R. Brooks, V. G. Young, Jr. and D. J. W. Grant, *Cryst. Growth Des.*, 20041, **4,** 1195 – 1201.

4 (a) B. Das and J. B. Baruah, *Cryst. Growth Des.*, 2011, **11**, 278-286; (b) X.-L. Zhang and X.-M. Chen, *Cryst. Growth Des.*, 2005, **5**, 617-622; (c) Ö. Almarsson and M. J. Zaworotko, *Chem. Commun.*, 2004, **17**, 1889 – 1896.

5 (a) C. C. Seaton, T. Munshi, S. E. Williams and I. J. Scowen, *CrystEngComm*, 2013, **15**, 5250 – 5260; (b) P. Sanphui, S. Tothadi, S. Ganguly and G. R. Desiraju, *Mol. Pharmaceutics*, 2013, **10**, 4687–4697.

6 S. R. Perumalla, E. Suresh, V. R. Pedireddi, *Angew. Chem., Int. Ed.,* 2005, **44**, 7752-7757.

7 (a) G. R. Desiraju, *Angew. Chem., Int. Ed.*, 2007, **46**, 8342–8356; (b) G. R. Desiraju, *Angew. Chem., Int. Ed. Engl.*, 1995, **34**, 2311-2327.

8 (a) V. R. Vangala, R. Mondal, C. K. Broder, J. A. K. Howard, G. R. Desiraju, *Cryst. Growth Des.*, 2005, **5**, 99-104; (b) V. R. Vangala, B. R. Bhogala, A. Dey, G. R. Desiraju, C. K. Broder, P. S. Smith, R. Mondal, J. A. K. Howard, C. C. J. Wilson, *Am. Chem. Soc.,* 2003, **125**, 14495-14509.

9 (a) B.-M. Ji, D.-S. Deng, N. Ma, S.-B. Miao, X.-G. Yang, L.-G. Ji and M. Du, *Cryst. Growth Des.*, 2010, **10**, 3060-3069; (b) T. Basu, H. A. Sparkes and R. Mondal, *Cryst. Growth Des.*, 2009, **09**, 5164-5175; (c) B. Sarma, N. K. Nath, B. R. Bhogala and A. Nangia, *Cryst. Growth Des.*, 2009, **09**, 1546-1557; (d) S. Kong, I. G. Shenderovich and M. V. Vener; *J. Phys. Chem. A*, 2010, **114**, 2393–2399; (e) I. Sarcevica, L. Orola, M. V. Veidis, A. Podjava and S. Belyakov, *Cryst. Growth Des.*, 2013, **13**, 1082-1090.

10 (a) I. D. Madura, K. Czerwiń ska, M. Jakubczyk, *Cryst. Growth Des.*, 2013, **13**, 5344-5352; (b) M. Du, Z.-H. Zhang, W. Guo and X.-J. Fu, *Cryst. Growth Des.*, 2009, **09**, 1655-1657; (c) L. Wang, L. Zhao, Y. Hu, W. Wang, R. Chen and Y. Yang, *CrystEngComm*, 2013, **15**, 2835–2852; (d) J. Ridout and M. R. Probert, *Cryst. Growth Des*., 2013, **13**, 1943-1948.

11 (a) C. B. Aakeröy, N. C. Schultheiss, A. Rajbanshi, J. Desper, and C. Moore, *Cryst. Growth Des.*, 2009, **9**, 432–441; (b) M. Du, Z.-H. Zhang, X.-G. Wang, H.-F. Wu and Q. Wang, *Cryst. Growth Des.*, 2006, **6**, 1867-1875.

12 (a) D. R. Weyna, T. Shattock, P. Vishweshwar and M. J. Zaworotko, *Cryst. Growth Des.*, 2009, **9**, 1106-1123; (b) S. Goswami, S. Jana, A. Hazra, H. K. Fun and Shazia Anjum, *CrystEngComm*, 2006, **8**, 712–718; (c) M. Du, X.-J. Jiang, X. Tan, Z.-H. Zhang and H. Cai, *CrystEngComm*, 2009, **11**, 454-462; (d) Z. Dega-Szafran, G. Dutkiewicz, Z. Kosturkiewicz, M. Szafran, *Journal of Molecular Structure*, 2009, **923**, 72–77; (e) B. Sarma, P. Sanphui and A. Nangia, *Cryst. Growth Des.*, 2010, **10**, 2388-2399; (f) L. Rajput, N. Jana, and K. Biradha, *Cryst. Growth Des.*, 2010, **10**, 4565-4570; (g) S. H. Dale, M. R. J. Elsegood, M. Hemmings and A. L. Wilkinson, *CrystEngComm*, 2004, **6**, 207–214; (h) J. Yang, Q. Yue, G.-D. Li, J.-J. Cao, G.-H. Li, and J.-S. Chen, *Inorganic Chemistry*, 2006, **45**, 2857-

2865; (i) A. Mallick, S. Saha, P. Pachfule, S. Roy and R. Banerjee, *J. Mater. Chem.*, 2010, **20**, 9073–9080.

13 (a) N. Shan, E. Batchelor, W. Jones, *Tetrahedron Lett.*, 2002, **43**, 8721-8725; (b) B. R. Bhogala, S. Basavoju, A. Nangia, *Cryst. Growth Des.*, 2005, **5**, 1683-1686.

14 S. Valiyaveettil, V. Enkelrnann and K. Mullen, J. Chem. Soc., Chem. Commun., 1994, 2097-2098.

15 (a) L. Wang, L. Zhao, R. Xue, X. Lu, Y. Wen and Y. Yang, *Sci. China Chem.,* 2012, **55**, 2515-2522; (b) L. Wang, L. Xu, R. Xue, X. Lu, R. Chen and X. Tao, *Sci. China Chem.,* 2012, **55**, 138-144; (c) L. Wang, R. Xue, L. Xu, X. Lu, R. Chen and X. Tao, *Sci. China Chem.,* 2012, **55**, 1228-1235; (d) L. Wang, L. Zhao, M. Liu, R. Chen, Y. Yang, Y. Gu, *Sci. China Chem.,* 2012, **55**, 2115-2122; (e) L. Wang, L. Zhao, W. Liu, R. Chen, Y. Gu and Y. Yang, *Sci. China Chem.,* 2012, **55**, 2381-2387; (f) L. Wang, L. Zhao, M. Liu, F. Liu, Q. Xiao, and Z. Hu, *Sci. China Chem.,* 2012, **55**, 2523-2531; (g) L. Wang, L. Zhao, L. Xu, R. Chen and Y. Yang, *CrystEngComm*, 2012, **14**, 6998-7008; (h) L. Wang, L. Zhao, Y. Hu, W. Wang, R. Chen and Y. Yang, *CrystEngComm*, 2013, **15**, 2835-2852; (i) L. Wang, Y. Hu, W. Wang, F. Liu and K. Huang, *CrystEngComm*, 2014, 16, 4142-4161.

16 (a) C. J. Burchell, C. Glidewell, A. J. Lough, G. Ferguson, *Acta Crystallogr., Sect. B*, 2001, 57, 201; (b) S. Mathew, G. Paul, K. Shivasankar, A. Choudhury, C. N. R. Rao, *J. Mol. Struct*., 2002, 641, 263; (c) D. M. M. Farrell, G. Ferguson, A. J. Lough, C. Glidewell, *Acta Crystallogr., Sect. C*, 2002, 58, 'o6'.

17 (a) A. D. Bond, *Chem. Commun*., 2003, 250-251; (b) A. D. Bond, *CrystEngComm*, 2006, 8, 333 – 337; (c) D. Braga, F. Grepioni and G. I. Lampronti, *CrystEngComm*, 2011, 13, 3122-3124.

18 (a) J. Lu and J. K. Kochi, *Cryst. Growth Des.*, 2009, **9**, 291-296; (b) D. R. Weyna, T. Shattock, P. Vishweshwar, M. J. Zaworotko, *Cryst. Growth Des.*, 2009, **9**, 1106-1123; (c) T. R. Shattock, K. K. Arora, P. Vishweshwar, M. J. Zaworotko, *Cryst. Growth Des.*, 2008, **8**, 4533-4545; (d) B. R. Sreekanth, P. Vishweshwar, K. Vyas, *Chem.Commun.*, 2007, **23**, 2375-2377.

19 SAINT Software Reference Manual, Bruker AXS: Madison, WI, 1998.

20 G. M. Sheldrick, SHELXTL NT Version 5.1. Program for Solution and Refinement of Crystal Structures: University of Gottingen, Germany, 1997.

21 Y. H. Deng, S. Y. Wang, J. Liu, Y. L. Yang, F. Zhang and H. W. Ma, *ACTA CHIMICA SINICA*, 2007, 65, 809-815.

22 (a) L. Brammer, *Chem. Soc. Rev.,* 2004, **33**, 476-489; (b) G. R. Desiraju, *Chem. Commun.,* 1997, 1475-1482; (c) G. R. Desiraju, *Angew. Chem. Int. Ed.*, 2007, **46**, 8342-8356.

23 (a) G. R. Desiraju, *Acc. Chem. Res*., 2002, **35**, 565-573.

